Pan African University
Institute of Water and Energy Sciences

PAN-AFRICAN UNIVERSITY

INSTITUTE OF WATER AND ENERGY SCIENCES

(*including CLIMATE CHANGE*)

Master Dissertation

Submitted in partial fulfillment of the requirement for the Master degree in

Water Engineering

Presented by

Thomas, Mutiso KAVOO

RAINFALL-INTENSITY DURATION FREQUENCY ANALYSIS AND PEAK-FLOW ESTIMATIONS FOR FLOOD RISK MANAGEMENT OPTIONS WITHIN GOUNTIYENA BASIN NIAMEY, NIGER.

Defended on 03/09/2019 Before the Following Committee:

Chair	Thameur Chaibi	Professor	National Institute for Research in Rural Eng. water and forestry
Supervisor	Bernhard Tischbein	Ph. D	ZEF, University of Bonn
External Examiner	Navneet Kumar	Ph. D	ZEF, University of Bonn
Internal Examiner	Bessedik Madani	Ph. D	University of Abou Bekr Belkaïd

Academic year 2018/2019

DECLARATION

I, Thomas Mutiso Kavoo, at this moment, declare that this thesis represents work realized to the best of my knowledge. Also, I declare that all materials, information, and results from other works presented here are fully cited and referenced in accordance with the academic rules and ethics

Signature — Date

Thomas Mutiso KAVOO — **15/09/2019**

Supervisors

This thesis has been submitted for the fulfillment of the requirements of the master of science, Water Engineering track from the Pan African University Institute of Water and Energy Sciences including climate change (PAUWES)

Signature — Date

Dr. Bernhard Tischbein — **17/09/2019**

Signature — Date 26/09/2019

Dr. Aymar, Y. Bossa

Signature — Date 26/09/2019

Dr. Jean HOUNKPE

ABSTRACT

Information on peak discharge and related probabilities is essential for engineering structure designs. Many basins are ungauged and therefore, data for statistical analyses are missing and input for sophisticated hydrological modeling is insufficient. Design storm estimations based on intensity duration frequency analysis and peak discharge estimations is an essential component for planning water management interventions. The study aims to contribute to flood risk reduction within the Gountiyena basin in Niamey/Niger through intensity duration frequency analysis and peak discharge estimations based on a 5-minutes interval rainfall from 1990 to 2017 for two stations. The Gumbel distribution was applied for the intensity duration frequency analysis while the Rational and the Soil Conservation Service-Curve Number methods were used for peak discharge estimations. Short rainfall durations produced high rainfall intensities with increasing return period. The intensities varied from 100mm/hr to 226mm/hr for both stations for 1-year and 50-years return period respectively. Estimated average peak discharges vary from 84m^3/s (1-year return period) to 290m^3/s (50-years return period). The results can serve as basis for decision making for planning water management interventions. Alternatives on appropriate flood management options were summarized and described.

Keywords: Intensity duration frequency analysis, peak discharge estimations, ungauged basin, flood management, water management interventions

RESUME

Les informations relatives aux débits de pointe et aux probabilités associées sont essentielles pour la conception des ouvrages d'ingénierie. De nombreux bassins ne sont pas jaugés et par conséquent, les données requises pour les analyses statistiques sont manquantes, de même que celles pour la modélisation hydrologique sont insuffisantes. Les estimations de pluie de conception basées sur une analyse des courbes intensité-durée- fréquence et des estimations de débit de pointe constituent un élément essentiel pour la planification et la gestion des ressources en eau. La présente étude vise à contribuer à la réduction des risques d'inondation dans le bassin de Gountiyena situé dans la ville de Niamey au Niger ; ceci à travers une analyse intensité-durée-fréquence et l'estimation des débits de pointe basés sur un intervalle de précipitations de 5 minutes de 1990 à 2017 pour deux stations. La distribution de Gumbel a été appliquée à l'analyse fréquentielle, tandis que les méthodes de calcul du nombre de courbes de service rationnel et de conservation du sol ont été utilisées pour les estimations des débits de pointe. Les courtes périodes de précipitations ont produit des intensités de précipitations élevées avec une période de retour croissante. Les intensités ont varié de 100 mm/h à 226mm/h pour les deux stations, respectivement pour une période de retour de 1 an et de 50 ans. Les débits de pointe moyens estimés vont de 84 m^3/s (période de retour d'un an) à 290 m^3/s (période de retour de 50 ans). Les résultats de cette étude peuvent servir de base à la prise de décision pour la planification des risques d'inondations et la gestion de l'eau. Des mesures de gestion des inondations ont été résumées et décrites.

Mots-clés : intensité-durée-fréquence, débits de pointe, bassin non jaugé, gestion des crues, gestion de l'eau

ACKNOWLEDGMENT

All glory and honor to the Lord God Almighty for enabling me this far; it is a dream come true. The work marks the ultimate peak of a journey that started steadily and developed to the colossal task. It would be unfair not to acknowledge everyone who in one way or another offered their support throughout the entire MSc study and research period. The brevity of this acknowledgment in any way does not downplay the enormous support I received from everybody mentioned or not mentioned in this section.

I express special thanks to the African Union Commission (AUC) for their trust and faith in awarding me this scholarship as well as the research grant that facilitated my studies and research. Special thanks to the Pan African University Institute of Water and Energy Sciences, including climate change staff and administration for presenting a pleasant schooling environment as well as facilitating my stay in Algeria. In a special way, I would like to thank African Monsoon Multidisciplinary Analysis - Coupling the Tropical Atmosphere and the Hydrological Cycle (AMMA-CATCH) and Institute of Research and Development (IRD) for their assistance and data provision.

My gratitude goes to my supervisors Dr. Bernhard Tischbein, Dr. Aymar Y. Bossa and Dr. Jean HOUNKPE, for their continuous guidance and support throughout the whole research period. My appreciation to the whole research team at the WASCAL competence centre Ouagadougou (Burkina Faso) and Niamey (Niger) not forgetting to mention Dr. Yacouba YIRA, Professor Boubacar IBRAHIM and Mr. Bouzed who contributed significantly in the development of this work. I would also thank especially my friends and colleagues for their support and encouragement throughout the research period.

I am grateful to my family for always standing by me. Despite the distance, their prayers, advice and motivation enabled me to push through, and I am grateful for their patience for all the period I have been away.

List of Tables

List of figures

List of Abbreviations

IDF – Intensity Duration Frequency

AMS – Annual maxima series

POT – Peak Over Threshold

CDF- Cumulative Distribution Function

PD – Probability Density

EDF – Empirical Distribution Function

GEV - Generalized Extreme Value

CWS – Canadian Weather Service

NWS – National Weather Service

SCS-CN – Soil Conservation Service – Curve Number

DEM – Digital Elevation Model

EM-DAT – Emergency Events Database

LULC – Landuse Landcover

HYSOGr – Hydrologic Soil Group

WMO- World Meteorological Organization

USSR – Union of Soviet Socialists Republicans (Soviet Union)

IAHS – International Association of Hydrological Science

AMC – Antecedent Moisture Content

FMMP – Flood Management Master Plan

IFM – Integrated Flood Management

ICZM – Integrated Coastal Zone Management

IWRM – Integrated Water Resources Management

CT – Continental Terminal

SRTM – Shuttle Radar Topographic Mission

LPT III – Log Pearson Type Three

EWS – Early Warning System

CHAPTER ONE

1 INTRODUCTION

1.1 Background

Flooding is one of the most devastating natural disasters. Despite the many efforts given towards flood management, its occurrence has always left visible and painful scars. In the last decade, flooding has affected over 7 million people, and property valued over 360 Billion (`000) USD destroyed (emdat, 2018). Cities are most affected by flooding due to their high population densities. Figure (1) below gives a global perspective of flooding for the last ten years from 2009 to 2019.

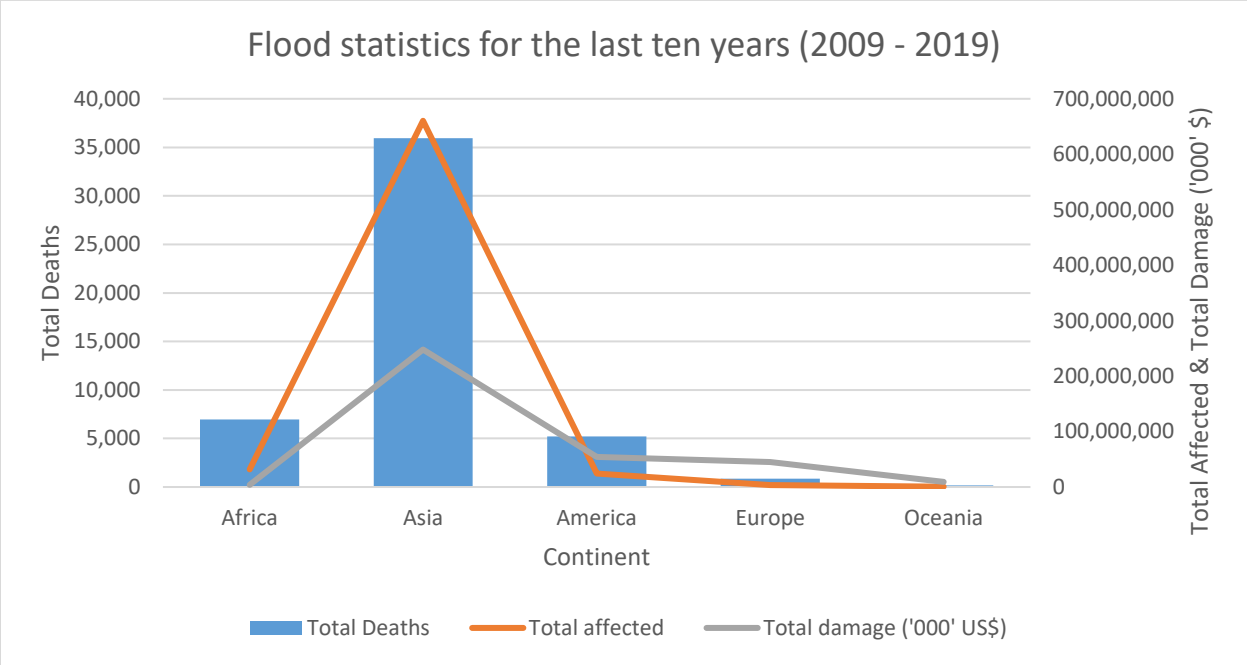

Figure 1: flood statistics for the last decade (2009 to 2019)

Urbanization is increasing rapidly due to the increased movement of people from rural to urban settings. It has resulted in the establishment of some of the largest cities in the world today. Cities have become social hubs, and life in cities is dependent on different services and utilities such as transport networks, electricity and water provision, education, housing, and employment. Any slight disruption on these utilities and services can cause a severe economic and social impact to both the city and the population. Urban flooding, a common phenomenon in the recent past can

affect these services and utilities, significantly leading to a severe negative impact on society. Recently, many notable flooding events are frequent.

The world`s population living in urban areas has surpassed the one in the rural areas, and projections indicate that the urban population will keep increasing as the world population shoots up (United Nation, 2018). The world`s population is expected to reach 8.6 by 2030 and more than 9.8 billion by 2050 from the current 7.6 billion people. Today, 55% of the total population live in urban areas, a figure which will reach 68% by 2050 (United Nations, 2017; United Nations, Department of Economic and Social Affairs, & Population Division, 2017). Rural to urban migration has led to the conversion of green areas into impervious layers leading to increased runoff generation. Also, due to the nature of most urban centers most often situated along with significant watercourses; most people live in flood plains, exposing themselves to higher flood risk.

Floods are natural disasters which are difficult to predict. Once floods happen, depending on the preparedness and risk mitigation measures in place, its impact varies from place to place. For cities to become flood resilient, there is a need for innovative and adaptable measures and strategies. Researchers agree that a resilient flood city will be least affected by flooding when it happens.

Therefore, in the wake of developing flood resilient cities or transforming our cities to be flood resilient, developers, planners, and engineers need to understand the severe impacts of flooding as well as understanding the reasons for flooding and the processes leading to floods (influenced by both natural and human-made factors. Flood impacts in the short run can include; loss of life, damage to property, destruction/interference with infrastructure (transport and electricity networks). Moreover, within the short to medium flood impacts, once contaminated floodwaters settle in a particular place for a prolonged time, they pose a health risk and can hamper the spread of diseases such as diarrhea and cholera and act as breeding places for mosquitoes which heightens the spread of malaria and dengue fever. Most importantly, flooding results in a significant economic impact, and this mostly affects the developing countries since they have fewer resources allocated to flood risk mitigation and recovery.

1.2 The statement of the problem

Niamey is a rapidly growing and developing metropolitan city. Initially sitting only on the left bank of Niger River, the city has grown and expanded now sitting on both banks of the river. Due

to massive migrations of people from the rural areas fueled by extreme events such as droughts mostly notable from the 1971 drought (Sivakumar, 1992). In the rainy season (May to August), drainage channels in the city flow in full capacity and places with insufficient drains, rainwater overflows from the channels and into the roads, and buildings. Anthropogenic activities and Climate Change transform the natural hydrological processes within catchments leading to amplified runoff generation with short peak time resulting to high discharge generation, low groundwater recharge and minimal soil moisture replenishment (H. Chang & Bonnette, 2014). Flooding in Niamey City is due to insufficient drains, stormwater planning, and inadequate inlet arrangements

Discharge data is vital for designing drainage systems in urban environments. Unfortunately, discharge and flood data for the study area is not available.

Just like many other urban basins, discharge and flood data is a big challenge, and engineers, urban planners, and developers usually rely on rough estimations during engineering structure designs. Un underestimation can lead to severe consequences which an overestimation can result in wastage and misuse of resources. In most cases, these critical decisions depend on historical events and their mode of occurrence. However, most of the structures already in place are of inadequate capacity or poorly managed. Urban floods are being experienced even with the slightest precipitation event.

With current climate projections depicting an increased frequency of extreme rainfall events, there is an urgent need to re-evaluate the existing structures, determine their capacity and if need be making the necessary adjustments in preparation of the known future. To make the right decisions, engineers, urban planners, and developers rely on existing discharge observations, flood data, and rainfall observations to make estimations and prediction of future events and their magnitudes. To get all these data sets is not easy. Therefore, whatever data is available is exhaustively utilized in determining the behavior of future events. Gountiyena is ungauged urban basin which has experienced frequent flooding events over the last decade. There is no discharge data or flood data available for the catchment. However, the basin has good records of rainfall data applicable for the development of regionalized intensity duration frequency analysis as well as peak discharge estimations. This research proposes to contribute to flood management through the development of intensity duration frequency (IDF) curves as well as determining peak discharges for different

rainfall intensities using the sub-hourly rainfall data. The gravity of this topic, as well as the existing research gaps, serves as the principal motivation for this research.

1.3 Research questions

1. What is the relationship between flood intensity, duration, and frequency in the Gountiyena Basin?
2. How can peak discharge necessary for flood infrastructure design be estimated for improved flood management in the ungauged basin of Gountiyena?
3. What are the current flood management options within the basin?

1.4 The study objectives

The main objective

The main aim is to contribute to flood risk reduction within the Gountiyena basin in Niamey through intensity duration frequency (IDF) analysis and peak discharge estimations.

Specific Objectives

1. To perform rainfall-intensity duration frequency analysis in Gountiyena basin
2. To estimate probable maximum peak discharges for a better flood infrastructure design in the ungauged basin of Gountiyena
3. To review current flood management practices applicable to the basin

1.5 The relevance of the study

The current study is going to improve flood management within the basin of Gountiyena and the entire city of Niamey. The developed results will serve as a basis for decision-makers such as urban planners, developers, disaster risk departments, and any other relevant stakeholder in the development of new infrastructures and the installation of flood management measures. Moreover, the current research results will be used to assess if the already existing flood management measures are adequate or they need improvement. It goes further to suggest new flood management options based on their effectiveness in other similar basins.

1.7 Chapter outline

The current study has eight chapters. Chapter one introduces the research by giving a comprehensive background on the study subject, research questions, problem statement, research objectives, and the relevance of the study. The concept upon which the research is based is amply expounded and justified as well as the structure of the study is also presented in chapter one. Chapter two gives a comprehensive review of the relevant literature on urban floods, intensity duration frequency analysis, peak discharge estimations for ungauged catchments, and best management practices towards flood risk reduction. Chapter three describes the study area; its location, weather, hydrology, geological settings, and data collection. The methodology applied to realize the study objectives are expounded in chapter four. The results and discussions of the research findings in chapter five. Chapter six gives the summary and implications of the key findings as well as recommendations and limitations of the study. Chapter seven contains the appendices of the additional attachments relevant to the study. The last chapter eight describes the references of all the works cited in this study.

CHAPTER TWO

2 LITERATURE REVIEW

2.1 Flooding

Flooding is one of the most frequent and destructive natural hazards globally significantly affecting lives and causing substantial economic loss (Khan et al., 2011). For several decades, the significant impact of anthropogenic activities on the hydrological cycle has received considerable attention. All over the world, many developments take place beside significant water bodies and their interference with the natural hydrological processes has resulted in remarkably stronger flooding events that are very unpredictable. Urbanization is said to have caused increased flood peaks and volumes(Tingsanchali, 2012).

In the rural settings especially in areas such as agricultural fields, processes of surface overland flow are comparatively not so complex to model generally determined by land cover, soil type and topography (A. M. Wasantha Lal, 1998). In urban areas, the case is different since processes of surface overland flow dominantly influenced by anthropogenic activities like storm drainage systems and land use. Urbanization leads to increased runoff generation and volumes because of a higher percentage of impervious areas such as roads, rooftops, and squares (Hsu, Chen, & Chang, 2000; Schmitt, Thomas, & Ettrich, 2004). Also, the direction of overland flow is altered artificially (potentially even against topography by pumping or artificial slope) by the construction of facilities such as buildings, roads, and drainage systems (Dawson et al., 2008). As a result, the behavior and generation of surface runoff in urban areas are quite different from rural areas.

Flooding occurs due to the quick accumulation of surface runoff from upstream to downstream resulting from heavy precipitation in a catchment. Discharges reach maximum very quickly and reduce as quickly as they form. According to Borga et al. (2010), flood occurrence is of great concern in hydrology and to the science of natural hazards because of its rank among natural disasters based on the global affected populations as well as the ration of individual mortalities. In many regions, flood causalities and damaging potential are increasing due to economic and social development, which indicates pressure on land use through development (Carlos E. M. Tucci, 2007).

Many researchers have contributed to urban hydrology, which has led to improved management of urban runoff for environmental protection, public health, and flood protection (Huong &

Pathirana, 2013). Significant advances have been noted recently in the prediction and measurement of urban precipitation. The capacity to predict urban hydrology has also progressed to give models appropriate to the small spatial and temporal scales distinctive of urban and semi-urban applications (Shepherd & Burian, 2003). Different models, therefore, have been developed to help address the increasing flood events in urban areas. Urban flooding is affecting both developed and developing countries. However, when it happens in developing countries, its impact on their economies is more devastating (Hammond, Chen, Djordjević, Butler, & Mark, 2015). Therefore, the current and future trend flood risk situations call for accurate temporal and spatial information regarding possible hazards and flood risks.

According to Chang (2006), high precipitation within an urban catchment results in floods. Urbanization brings about the conversion of natural vegetation, wetlands, and agricultural lands into built-up environments and construction atop natural drainage channels and increase of population of persons living in flood-prone areas like floodplains and watercourses. Hydrological characteristics such as reduced infiltration, increased surface runoff generation, and increased frequency and flood magnitude have a direct relationship with urbanization. Urban areas are more vulnerable to flood risk due to their unique characteristics such as high population, diverse economic activities, several infrastructure and developments which generally affect the natural infiltration process.

Small streams of developed areas rise quickly after a rainfall event because of higher runoff generation with very little concentration time. Alterations in an urban area and rainfall intensity generates higher flows that exceed the capacity of the small drainage channels along the roads designed for non-developed areas. Many structure designs are based on probability and can sustain an event of a specific magnitude. However, during extreme events, their capacities are inadequate leading to flooding. In most developing countries, the situation aggravated by poor maintenance of drainage channels, disposal of solid waste, and debris into the channels (Ouma & Tateishi, 2014). It is imperative to understand that the rainfall-runoff process is exceptionally complex, non-linear, and spatially and temporally changing due to terrain variability and climate change.

Even though these structures might be sufficient when adequately designed, their capacities might be inadequate during extremes resulting in floods in the developed areas. In most developing countries, the situation aggravated by poor maintenance of drainage channels, disposal of solid

waste, and debris into the channels (Ouma & Tateishi, 2014). It is imperative to understand that the rainfall-runoff process is exceptionally complex, non-linear, and spatially and temporally changing due to terrain variability and climate change.

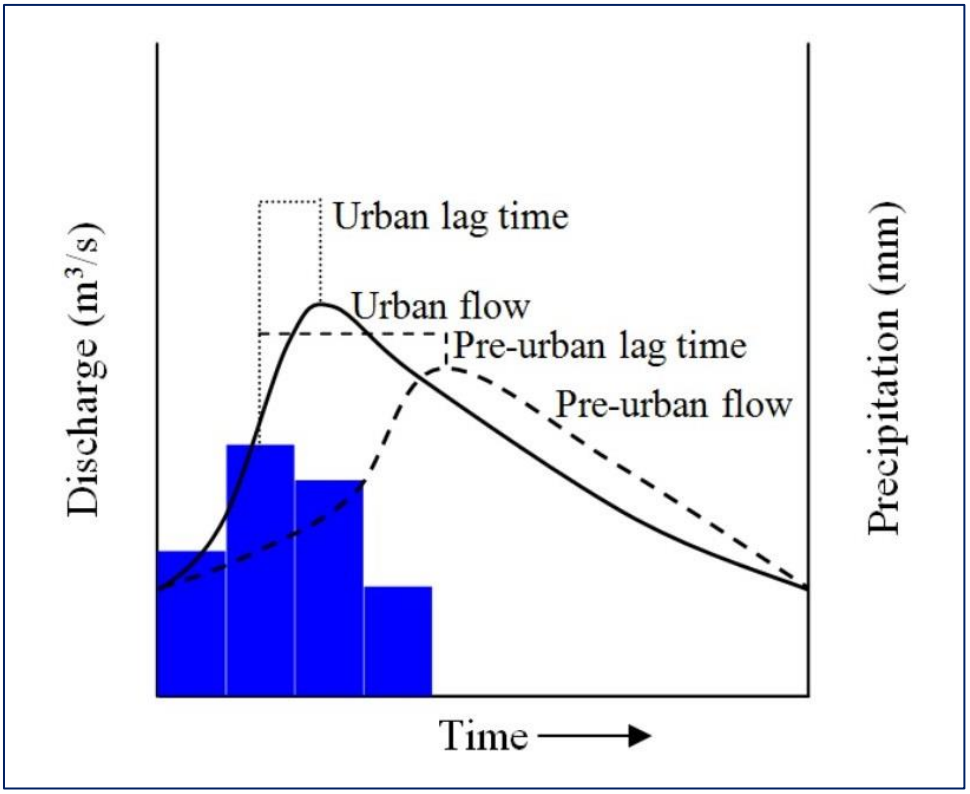

Figure 2: Urban and non-urban area typical Hydrograph **(Source: Ouma & Tateishi, 2014)**

2.1.1 The Impact of urban infrastructure

Once an urban center develops, the whole ecosystem of the area transforms. Green areas are replaced with impervious layers minimizing the amount of infiltrating and percolating water and on the other hand, increasing runoff generation. In developing countries, urbanization results in large population concentration in a small area limited to water supply, transport network, and sanitation and suffered from flooding, polluted water, and air.

Moreover, these urban centers have uncontrolled growth. Also, many people who migrate to urban centers from rural areas quite often end up living in flood-prone areas such as in the floodplains. People always hope for better lives in the cities, and there is a massive rural-urban migration. Rural-urban migration is high, precisely due to the availability and accessibility of many public services. Also, urban growth is spontaneous, and urban planning is only limited to the parts of the

city occupied by the high income and middle-class population. Developers often ignore spatial planning, and they end up building houses in areas with a risk of flooding, landslides, and other associated natural disasters leading to recurrent deaths every rainy season. For instance, over 100 deaths were reported due to flooding in Niger and properties worth 10, 000 ('000' USD) lost.

According to Tucci (2007), urbanization problems have increased currently because:-

- Majority of the population moving to cities are struggling financially and do not have any investment capacity, and they majorly migrate in the hope of getting better lives in the urban areas and end up invading public areas or purchase of marginalized areas with limited infrastructures and at risk of flooding.
- Poor planning and lack of urban settlement policies
- High incomes due to high employment rates as compared to rural settings but with housing deficits
- Lack of capacity for the municipalities to plan and anticipate urban growth as well as investing in planning for safe and appropriate spaces for development.
- Many developing areas suffer an economic crisis with their budget allocations mainly guided by other pressing issues like education, food, and health care.
- Many municipalities in developing countries have inadequate resources and therefore, only manage to implement land-use regulations in the formal city with intermediate and high economic values.

2.2 Intensity duration frequency (IDF) analysis

The environment has a direct impact on human lives, be it positive or negative. Severe environmental events like; storms, floods, droughts, and high catastrophic winds have dire consequences on the population. According to Hosking & Wallis (1997), Planning and preparation for emergencies due to weather, engineering structure designs, pollution control, reservoir management, and insurance risk calculations are all dependent on the frequency of these extreme weather events. The evaluation of these extreme precipitation events is a critical problem in risk analysis and design in hydrology. Rainfall extremes evaluation, as represented in intensity-duration frequency analysis relationship, has drawn significant attention for both applied and theoretical hydrology (Veneziano, Langousis, & Furcolo, 2006). Intensity-duration rainfall frequency analysis refers to the graphical representation of rainfall amount falling within a specific

period (Dupont & Allen, 2000). The graphs symbolize when it is likely to flood as well as when likely is the same amount of rainfall reoccurring in the future.

The intensity duration frequency relationship is fundamental, especially when designing systems for handling (urban) storm runoff such as; culverts, roads and drainage systems (Hoblit, Zelinka, Castello, & Curtis, n.d.). According to Maidment (1996), rainfall frequency analysis challenge is the computation of the rainfall amount falling over a specific area within a given time (in minutes) with a given occurrence probability in any specified year. However, for the application of IDF in engineering design, the temporal rainfall distribution of a given frequency should be specified or its return interval defined. The IDF curves provide for the determination of the average rainfall depth of a given exceedance probability spread over a range of periods resulting from the rainfall frequency analysis (Maidment, 1996). The hydrologic engineering design heavily relies on the IDF estimates, vital statistical precipitation records summaries (Gerold & David W. Watkins, 2005).

The development and application of the IDF Relationships date back as early as 1928 (Meyer, 1928). After Meyer brought the IDF idea and had developed a number of them, a general intensity duration formula was developed by Sherman (1931) while Bernard (1932) made accessible for locations within the limits of the study for 5, 10, 15, 25, 50, and 100 rainfall intensity frequencies for 120 to 6000 minutes rainfall duration. Bell developed an IDF relationship through the application of a formula that enabled the computation of the depth-duration ratio for a specific area of the Soviet Union (U.S.S.R) in 1969. In Africa, IDF curves for various cities in Ghana and Nigeria were developed J. B Danquah 1972 and Oyebande 1982, respectively. A simple method for the derivation of comprehensive rainfall intensity duration frequency for the United States of America was developed by Chen in 1983 using isopluvial maps (Technical paper 40 of the United States of America) (Hodges, Hershfield, Washington, & Reichelderfer, 1961)

The development of IDF relationships birthed some consistent mathematical approaches in the 1990s. A mathematical model for modeling extreme storm probabilities from the scaling attributes of precipitation station observed data together with multiple and straightforward scaling estimations was introduced to describe extreme rainfall event temporal structure (Burlando & Rosso, 1996).

Further developments by Koutsoyiannis (1994, 1996 and 1998) led to the development of a new approach to the design and development of IDF Curves using both recording and non-recording

stations data. According to Koutsoyiannis, the approach explains a general but yet thorough approach for IDF relationships generated from the first probability distribution function of the maximum intensities. Also, he proposed two IDF Relationships parameter estimation methods.

Recent studies have applied statistical distributions and realized that the Gumbel Extreme Value Distribution fitted well to the data (García-Bartual & Schneider, 2001). A Rainfall Intensity Frequency relationship for non-recording stations grounded on the scaling approach that applies the hypothesis of piecewise easy scaling coupled with Gumbel Distribution (Yu, Yang, & Lin, 2004). In other developments, IDF Curves have been combined and analyzed together in generating design rainfall estimation for short storm durations (less than an hour).

Based on the IDF approach presented by (Koutsoyiannis, Kozonis, & Manetas, 1998), Karahan (2007) estimated the parameters for the same using a genetic algorithm. The development of IDF Curves is possible through the application of bivariate precipitation frequency analysis through the application of the Frank Archimedian Copula Method (Singh & Zhang, 2007; Zhang, 2009). Mohymont, Demarée, & Faka, (2004) performed an assessment of Intensity Duration Frequency Curves for stations located in Central Africa and suggested the application of physically models for the development of IDF curves. Depending on their application, IDF curves can be developed with different time steps from maximum sub-daily rainfall intensities to weekly, monthly, and annual rainfall intensities. According to Langousis & Veneziano, (2007), if $I(d)$ is the mean rainfall intensity for a duration time (d), then $I_{max}(d)$ is annual maximum of $I(d)$ and $I_{max}(d, T)$ depicts the value exceeded by $I_{max}(d)$ on the mean of every T years. The IDF Curve relationship is then plotted as the I_{max} against d for different T values. In the recent past, there have been increased IDF curves demands. The reasons for the increased demand can be summed as follows;

- Urbanization leads to increased surface sealing leading to increased runoff generation rendering the natural drainage channel inadequate. To understand the full extent of this inadequacy needs information regarding extreme rainfall events with which drainage works have to resist
- With increased understanding and documentation of the spatial heterogeneity of the extreme rainfall events, there is an urge for the value of the regionally applicable IDF information

- Climate change projections are indicating an increased intensity and frequency of extreme rainfall events. Therefore, IDF values will optimally require frequent updating in the future than in the past using different climate change scenarios

2.2.1 The IDF curves characteristics

The Intensity Duration Frequency Curves have a unique characteristic that defines their nature. In a logarithmic coordinate system, the IDF correlations present an almost parallel reducing line. These lines cannot cut across each. For all the return periods, it is possible to determine rainfall intensity for all given rainfall durations. Every return period gives high rainfall intensities for short rainfall duration.

2.2.2 Methods for deriving intensity duration frequency curves

In his review regarding IDF curves derivations methods, Koutsoyiannis (2004) presented three distinct methods for developing Intensity Duration Frequency Curves.

The first approach illustrates that for a recurrence interval *(T)* that is below the observed data length, IDF curves can be directly estimated using the annual maximum rainfall through the application of the plotting-position formula. The plotting-position method generates a non-smooth curve. However, only in a few circumstances when the long continuous data is available has this been considered as a feasible alternative.

In most cases, long observation records are available for daily rainfall data. Therefore, the experimental IDF Values (where *d = 1 day)* are applied IDF calibration procedure using alternative approaches or in constraining the dependencies of *id, T on T* (Koutsoyiannis, 2004; Mohymont et al., 2004).

The second approach and one of the most widely applied IDF curve development applies a parametric model for the rainfall intensity (*id, T).* In this approach, the reliance on *d* is founded on the characteristic shape of the experimental IDF curve, whereas the use of *T* depends on the fact that rainfall maxima are more attracted to the extreme distribution types. This approach applies models, and these models require several parameters to function effectively. The estimation of the model parameters is done using the observed data of extreme annual events. There are different methods available for parameter estimation and such includes; maximum likelihood, moment matching, and least square (Koutsoyiannis et al., 1998). IDF parameters lie in two distinct categories;

The ones of the function *a(T) (with κ, λ, and Ψ among others based on the selected distribution method)* where; *κ* - shape parameters, *λ* - scale parameters and *Ψ* - Location parameters and those of the *b(d)* function with η and Θ parameters (Koutsoyiannis et al., 1998). *T* and *d* stand for recurrence interval and rainfall duration, respectively.

According to Koutsoyiannis et al. (1998), and based on the reviewed procedures, he assumes *k* groups and each holds historical rainfall intensities of a given duration d_j, *j=1, k* denoted as n_j with the length of each group as *j* and by i_{j1} as the density values for that specific group. The samples of the given random variables $I_j = I(d_j)$ and with $I = 1, \ldots, n_j$ expressing the i_{j1} value rank of the group *j* organized in descending order. Chow et al. (1988), developed IDF curves parameters estimation procedure with three distinct steps as described below;

1) For each group, fitting of the probability distribution function (PDF) is made up of data values of a given duration d_j.
2) Rainfall intensities for every rainfall duration together with an identified return periods such as; 2, 5, 10, 25, 50, 100, and 1000 are computed using the selected PDF in step one.
3) Lastly, the Intensity Duration Frequency Curves can be obtained using two approaches;
    a. For every identified return period, rainfall intensities in step 2 help to establish a relation of intensity (*i)* as a function of duration (*d)* (expressed as $i=i_d(d))$ using bivariate least-square procedures and
    b. Intensities in step 2 for the identified return periods can be treated simultaneously to generate a relationship of *i* as a function of *d* and *T* (expressed as *i=I (T, d))* using three-variate least square procedure.

Chow et al. (1988) parameter estimation procedure`s main advantage is its ease of computation. The method subdivides the calculations into three steps, and each step has less clumsy procedures. However, just like many other methods, the procedure has its weakness which includes;

a) The procedure applies an experimentally derived function *a (T)* rather than using the function consistent with the selected probability function in step one.
b) Chow`s procedure is subjective in that the final parameters entirely depend on the return periods, as shown in step two. However, this dependence might be meaningful if the chosen empirical function *a (T)* leaves considerably from the one implied by probability distribution function (Koutsoyiannis & Manetas, 1996)

c) The procedure treats all the variables *I, d, and T* as ones with the same nature without taking into consideration that they are all different in that; *I denotes random variable, d is a non-random variable and T is the change of the PDF of the random variable.*

To address these inadequacies, its recommended to apply the third method that involves fitting an entire model of temporal rainfall to that of continuous rainfall records and then apply the model in generating rainfall time series using the Monte Carlo Simulation. IDF Curves generated using models are smoother than experimentally developed ones and have an estimated validity that goes beyond the given range of the historical data. When using a model to develop an IDF Curve, the application of the available data uses no assumption whatsoever of the IDF curves. However, this approach is less applied despite its ability to give satisfactory results due to its complexities in rainfall models formulation, parameter estimation, and the generation of the Monte Carlo Samples. The complex structure and the intense rainfall model parameterization more so those point-based processes make the application of this method practically impossible. However, there is hope this method will become simpler through the ongoing research on the extreme rainfall events.

This work applies the second approach proposed by Chow in developing IDF relationships. Despite its weaknesses, the approach is accepted globally and yields satisfactory results more so when applied in a small watershed. The parameters for the selected distribution method will be estimated using the moment matching procedure.

2.2.3 Frequency analysis theoretic principles

- **Fitting probability distribution to data**

Quantitative data has two general categories; experimental and historical. Experimental data usually measured through experiments is obtained frequently via experiments whenever required. On the other hand, historical data refers to data collected from a natural event observed only once and will not occur again. Once historical data is lost, it is difficult to retrieve. Hydrological data is considered historical and easily manipulated using statistical variables.

One of the most significant challenges facing many hydrologists is the lack of historical data. Many basins are still ungauged, and some that are ungauged have very scanty data available with plenty of missing data. It is challenging for hydrologists to collect and store all hydrological data such as discharge and precipitation data. When a decision has been reached to perform any water-related

project in a specific area, it is necessary to identify, and collect all the information relating to the area as well as analyzing the collected data. For hydrological data, a Frequency Analysis of the collected data is the most commonly applied method.

The available data is characterized using a numerical model which also aids in filling the missing data or in extending the observed records to a more extended period. The characterization is essential as it ensures consistency of the observed hydrological data available. Fill the missing data can be achieved sometimes through using correlated data gotten from hydrological areas located geographically closer and comparable to the study area or through the application of the historical values. The period of the observed data can be prolonged using a model. Even though hydrological values are continuous, they are discretized and utilized as discrete series.

The frequency analysis of hydrological data is performed using probability distribution functions and is done to link extreme storm events to their occurrence frequency. In most cases, hydrological variables are assumed to have a specific distribution type. Some of the commonly applied distribution types in hydrology include; Normal, Log-normal, Gamma, Exponential, Pearson type I, II, and III, Log-Pearson, General Extreme Value I (Gumbel), General Extreme Value II, and General Extreme Value III (Weibull).

The normal and log-normal probability distributions generally fit into the annual river flows. The Gamma distribution has the advantage in hydrology in that it only gives positive values, and we know that hydrological variables (precipitation and Discharge) are consistently positive.

The Gumbel and the Weibull Probability Distributions are applied for extreme maximum and minimum values respectively for hydrological variables. The Gumbel is applied in frequency analysis of floods, while the Weibull distribution in the frequency analysis for low flows observed in a river channel.

The current study applied the methods of moments method in estimating the probability distribution parameters. The method has been applied in the development of the Intensity Duration Frequency by many hydrologists and meteorologist globally such as; Canadian Weather Service (CWS), National Weather Service (NWS) USA, United Kingdom, Ghana, and Nigeria.

Many probability distributions functions do not exist individually but as a family of many distributions. The reason for this is basically because some distributions have one or several shape

parameters. The shape parameter allows distribution to take different shapes depending on its shape parameter value. Such distributions are significant, especially when modeling applications since they are highly flexible to model diversified data sets.

2.2.4 The probability distribution of extreme hydrology variables

a) The exponential distribution

Some hydrological event sequences, the likes of precipitation occurrence are a Poisson process in which occurrence of events is instantaneously and independent on a time horizon. The time interval between such events is illustrated by exponential distribution whose λ parameter is the average rate of events occurring. This distribution type applies in describing inter-arrivals times of the random shocks to hydrologic systems like polluted runoff slugs discharging into a stream as precipitation washes the pollutants off the surface. The main exponential advantage is its ease of use in estimating the λ from the observed records, and it presents itself best for theoretical studies like in the probability model for a linear reservoir where

$$\lambda = \frac{1}{k}$$

where; k: storage constant of the reservoir.

The method has the main weakness in that it needs occurrence of every event to be completely independent of its neighbors a situation difficult to experience, thus an invalid assumption for the study process.

b) Gamma distribution

In a Poisson process, the Gamma distribution determines the time taken by several β events to occur. The Gamma distribution is a distribution of the sum of β independent and similar exponentially random distributed variables. The distribution has a smoothly changing form similar to the typical distribution density function and is very significant for explaining skewed hydrologic variables without subjecting them to log transformations. The method is used to explain the distribution of precipitation depth in storms. It applies the Gamma function r(β) given by;

$$r(\beta) = (\beta - 1)! = (\beta - 1)(\beta - 2)$$

Equation 2-1

$$\Gamma(\boldsymbol{\beta}) = \int_{\mathbf{0}}^{\infty} \boldsymbol{u^{\beta-1}e^{-u}du}$$

Equation 2-2

The two-parameter Gamma Distribution (β and λ) has its lower bounds at zero. Lower bound values greater than zero is a disadvantage for its application to hydrological The IDF analysis uses the Maximum Intensity values with lower bound values larger than zero hence limiting the Gamma Distribution application in IDF analysis.

c) The Pearson type III distribution

Also known as the three-parameter Gamma distribution introduces a third parameter known as the lower bound ϵ. The lower bound ϵ means that by the moment's method, it is easy to transform the three sample moments (i.e., mean, standard deviation and Skewness coefficient) into three parameters β, λ, and ϵ of the probability distribution.

The Pearson type III distribution is highly flexible with the assumption that the number of different shapes varies. The distribution method has seven types all solutions to the *f(x)* function in an equation of the form;

$$\frac{d[f(x)]}{dx} = \frac{f(x)(x-d)}{C_0 + C_1 + C_2x^2}$$

Equation 2-3

Where; d: distribution mode for the value of x for which f(x) is maximum while C_0, C_1, and C_2 are the missing coefficients. When the values of $C_2$is equals to zero, then the solution of the equation (2-3) above is Pearson Type III Distribution.

Foster introduced the application of the Pearson Type III Distribution in 1974 by describing the probability distribution of the annual maximum flood peaks. However, the method has a significant weakness when the data is positively skewed.

d) The Log-Pearson type III probability distribution

When *X* follows a Pearson Type III Distribution, it is also said to follow a Log- Pearson Type III Distribution. The log- Pearson Type III Distribution is the standard distribution for the annual maximum flood frequency analysis for the United States of America.

The location of the lower bound ϵ in the Log-Pearson Type III Distribution is dependent on the data skewness. The major setback of this methods is if the data are skewed positively, then $logx \geq \in$ and $\in$ represents the lower boundary and for a negatively skewed data, then $logx \leq \in$ and $\in$ represents the upper boundary.

The logarithmic transformations minimize the skewness of the transformed data and may lead to the generation of a transformed data skewed negatively from the observed positively skewed data. In such instances, the Log-Pearson Type III distribution imposes an artificial upper boundary on the data. Finally, the method requires large data samples to develop the shape parameters value β, λ, and ϵ of the distribution.

e) The Gumbel extreme value distribution

The extreme maximum and minimum values data sets are selected. In a given location, the annual maximum discharge measurements refer to the highest recorded value within a year. When the number of maximum values is from historical discharge measurements, it yields extreme values that can be statistically analyzed.

The distribution of extreme values from sets of samples of any distribution join to one of the three extreme value probability distribution referred to types; I, II and III for large selected extreme values. The three limiting methods are exceptional cases of sole distribution known as the General Extreme Value (GEV) Distribution with the following function;

$$f(x) = exp\left[-(1 - k\frac{x-u}{\alpha})^{1/k}\right]$$

Equation 2-4

Where k, μ, and α denotes the parameters to be estimated. The three limiting cases for the GEV distributions included;

- For values of k=0, Type I Extreme Value Distribution.

- For values of k<0, Type II Extreme distribution and in which the equation (2-4) applies

$$(u + \frac{\alpha}{k}) \leq x \leq \infty$$

- For values k>0, Type III Extreme value distribution in which equation (2-4) applies for the following relationship;

$$-\infty \leq x \leq u + \alpha/k$$

All three cases assume that α is positive. The three EV bounds include;

- Type I distribution, *x* is unbounded
- Type II, *x* is bounded from below by u+α/k
- Type III, *x* is bounded from above by the relation u+α/k

Type I Extreme Value Distribution is referred to as the Gumbel while Type II is known as the Frechet distributions. On the other hand, when type III Extreme Value Distribution describes a variable x, then -*x* is considered as having the Weibull Distribution.

The extreme value distributions (Type; I, II, and III) have three asymptotic forms. The EV I probability Distribution Function is presented as;

$$f(x) = exp\left[-(-\exp\left(-\frac{x-u}{\alpha}\right)\right] \text{ For } -\infty \leq x \leq \infty$$

Equation 2-5

To compute the α and μ parameters;

$$\alpha = \frac{\sqrt{6}s}{\pi}$$

Equation 2-6

$$\boldsymbol{u = \bar{x} - 0.5772 \propto}$$

Equation 2-7

The mode of the distribution of parameter *u* is known as the point of the maximum probability density and reduced *y* variate is;

$$y = \frac{x - u}{\propto}$$

Equation 2-8

If we substitute the reduced variate into equation (2-5), we form;

$$f(x) = exp[-exp(-y)]$$

Equation 2-9

Also, to solve for *y*, we apply the following relation

$$y = -\ln\left[\ln\left(\frac{1}{f(x)}\right)\right]$$

Equation 2-10

The relation presented in equation (2-10) can define *y* for Type II and type III EV distributions.

The generated values *x and y* can be presented graphically. Type I EV distribution produces a straight-line plot for large *y* values. The EV Type II distribution presents steeper slopes as compared to type I whereas the Type III distribution slopes are less steep and have an upper bound. EV distributions have a wide application in hydrology. In Great Britain, EV distributions form the standardized flood frequency analysis techniques. Generally, extreme rainfall events are modeled using type I distribution while droughts or minimal flows are modeled using the EV type III (Weibull Distribution).

The rainfall records applied in this study fit to type I (Gumbel) Distribution. The most common and widely used distributions are the Gumbel and Log-Pearson for frequency analysis of the extreme-maximum values. The Gumbel distribution is a two parametric function and is more advantageous than the Log-Pearson distribution in that it does not require large data sets in estimating all the parameters. It is highly recommended for individual gauge records frequency analysis since the data might not be adequate in determining the shape parameter.

- **The Gumbel distribution**

The Gumbel Distribution is a Probability Distribution Function applied in forecasting extreme hydrological events like floods. The Method has been extensively in flood forecasting in the United Kingdom as well as in many other parts of the world. In hydrology, a random variable is

said to obey a Gumbel Distribution if its cumulative Distribution Function (CDF) and Probability Density (PD) follow the form;

$$f(x) = exp\left[-(-\exp\left(-\frac{x-x_0}{s}\right)\right] \text{ For } s \neq 0$$

Equation 2-11

$$f(x) = \frac{1}{s} exp\left[-\frac{x-x_0}{s} - \exp\left(-\frac{x-x_0}{s}\right)\right]$$

Equation 2-12

$$-\infty < \boldsymbol{x} < +\infty;\ -\infty < \boldsymbol{x_0} < +\infty; \boldsymbol{s} > \mathbf{0}$$

Where; s: Scale parameter and

X_0: Position Parameter

If we apply the transformation function $u = \frac{x-x_0}{s}$ the Type I Extreme Distribution (Gumbel) is;

$$f(u) = \exp[-\exp(-u)]$$

Equation 2-13

$$f(u) = \exp[-\mu - \exp(-u)]$$

Equation 2-14

The transformed CDF is useful only when defining given frequency quantiles or return periods for extreme rainfall events like floods peaks; the annual maximum rainfall, which leads to the generation of maximum annual flows.

2.2.5 Testing of goodness-of-fit

The determination of the validity of the probability distribution fitting is through the goodness-of-fit test. Performing the statistical goodness-of-fit test or the graphical display (probability plots) are applicable ways of determining if the selected distributions agree with the observation data sets. Most importantly, the model selection is not only based on the fitting, but its predictive ability is fundamental, mainly when predicting future events.

When selecting a distribution, sometimes one is lured to selecting one that has many parameters. The more parameters a distribution have, the better the fitting of the data. However, the challenges presented during the parameter's estimation and worse enough, the distribution might be too rigid to extrapolate accurately beyond the span of the available data.

The goodness-of-fit test has three major classes; probability transformation tests, Regression type tests, and the Special features test. The most used Regression testing method is the probability plotting that involves plotting the ordered sample data on a graph with transformed axes so as the data to obey to the selected distribution; lying on a straight line. When plotted, it is easy to assess non-conformity visually. Goodness-of-fit tests should always be amplified using a probability plot. The relative frequencies of sample data together with the fitted pdf is plotted on the same graph to perform an informal visual test of the data.

The Chi-Square goodness-of-fit, one of the oldest, has the least subjective comparison of the frequency histograms with the fitted distributions. The Chi-Square test procedure divides the sample data into a discrete number of intervals and then compares the number of data points falling in each interval with the expected, predicted number of the fitted distribution. Integrating the fitted distribution between boundary interval and then multiplying by data points number in the sample yields the expected number. Even though this procedure is applicable for continuous variables, its application is more accurate categorical and arithmetically discrete random variables. Continuous random variables have infinite ways to portioning the support of the variable and do not have a unique interval number choice. However, even though the method is less subjective as compared to the visual assessment, it is not entirely objective.

Probability transformation tests develop on the fact; if a data set obeys a probability distribution, *f(x)*, the transformed variable y_i is usually given by $y_i = \int_{-\infty}^{x_i} f(x)dx$ obeys a uniform distribution. The statistic tests (Kuiper, Kolmogorov-Smirnov, Cramer-von Mises & Anderson Darling) are all measures of sample deviation from uniformity. The Kolmogorov statistic test determines the maximum deviation the transformed ordered variable above or below the smooth line. Kuiper statistic tests are the total sum of the maximum deviations from both sides of the uniformity line (above and below). The Cramer-Von statistic procedure is the sum of the squared deviations uniformity line and the Anderson-Darling statistic tests the weighted sum of the deviations with emphasis on the observations in the distribution tails.

In hydrology, both the Anderson-Darlin and Cramer-Van Mises tests are not prevalent may be due to some complexities that unavoidably emerge when the hypothetical distribution parameters are unknown, a pervasive case in hydrology. For the case where the parameters are entirely determined a priori, the Distribution of the EDF test statistics depends on the null hypothesis. The computation of the percentage points$100(1-\propto)$ (where $\propto$ is the level of significance of the test) percentiles of the tests statistics distribution come for all the null hypothesis.

Parameter estimation methods, shape parameter presence, and sample size have a more significant impact on the percentage points further complicating the analysis. This study applies the two prevalent and straightforward goodness-of-fit tests in hydrology (Kolmogorov-Smirnov and the Chi-Square tests)

2.3 Synthetic methods for runoff estimations within ungauged basins

Hydrological simulations within ungauged basins face numerous challenges. Apart from the primary challenge of lack of data; interpreting uncertainties due to these predictions is another major challenge (be it from climatic inputs, soils, land use, vegetation or from the model applied) in simulating the predictions (Sivapalan, Blöschl, Zhang, & Vertessy, 2003). The historical fragmentation of methods and approaches in a crafting ungauged basin prediction is a big challenge. There are research disagreements rather than agreements within the hydrologic community (Hrachowitz et al., 2013). Many hydrologists argue that greediness of most hydrological models applied in the field globally is a significant division indicator in the hydrological field (G. Clark, 2016).

Surface runoff is one of the fundamental components of the hydrological cycle difficult to ignore in any hydrological analysis. It affects the design and performance of every hydraulic structure. It is therefore essential to know the amount of volume and rate of direct runoff from a catchment. Within a gauged catchment, this data comes from hydrometric stations. On the other hand, obtaining discharge data for ungauged catchment is a challenge. Runoff estimation provides general information regarding a basin runoff potential, soil and water management and planning and for flood risk analysis (Andrea et al. 2017). Many synthetic discharge estimation methods have evolved in literature for runoff estimations in ungauged basins depending mainly on the climatic and physiographic conditions of the basin (Mishra and Singh, 2003; Lal, 2015; Sudhakar *et al.*, 2016).

The Rational, the Soil Conservation Service – Curve Number (SCS – CN), The Cooks, and the Hydrograph methods are the most common runoff estimation methods (Sudhakar *et al.*, 2016). Xiao *et al.* (2011) and Lal (2015) also highlights the SCS – CN method as the most common method. The SCS-CN method has been used to compute discharge data for many hydrological modeling including but not limited to; stormwater modeling, water resources management and estimation of runoff for a single rainfall event in small agricultural or urban watersheds due to its ease of use and minimal data requirement.

2.3.1 The Rational method

The rational method is among the most widely applied runoff estimation methods for a single storm event. The method is applied globally for different basin (Petroselli & Grimaldi, 2018). It has given outstanding results for small-sized basins up to 100 acres and a good result for larger basins up to $2mi^2$ basins (Dhakal, Fang, Thompson, & Cleveland, 2014). The method applies an empirical linear equation for peak runoff computation from an identified period of homogeneous rainfall intensity. It has been in existence for over a century and still very useful and relevant for peak discharge estimation from simple and relatively small drainage basins.

The application of the Rational Method should only be limited to drainage basins of less than or equal to 100 acres with similar surface topography and surface cover. This method can only be applied in computing peak discharge only since it is not based on the entire storm duration but rather on the storm period that produces the peak discharge (Petroselli & Grimaldi, 2018). However, for runoff volumes, the method can be applied, but it has to factor in the whole storm duration. It is best suited for small urban basins without detention ponds or swamps.

The application of the rational method uses a simple equation that links the discharge generation potential of the basin, the runoff coefficient, average rainfall intensity for a specific period (Concentration Time) and the Basin Area (Chen, Yue, Cui, & Li, 2007).

The Rational method has been extensively applied to estimate peak discharges of many ungauged basins for different design purposes like in the design of highways and drainage channels. According to NASH (2007), the origin of the rational method is uncertain. However, its application is dated as back as 1851. In their study, Hotchkiss & McCallum (1995) reviewed different peak discharge estimations methods for small ungauged basins for the Nebraska region, including; Fletcher method, Statewide regression formulae, and the rational method. In their review, the

results indicated a close relationship between the computed discharges for the above mentioned three methods. The rational method was applied to compute peak flows for the design of infiltration structures (Akan, 2002). The method was applied to estimate the peak flow of a landslide-induced flow in china (Chen et al., 2007)

2.3.2 The Envelope curve method

The Envelop Curve is another method of peak flow estimation developed by Creager Justin and Hinds from the United States of America. The method uses the assumption that the highest known discharge per unit area observed in the past in a specific basin is likely to occur in the future in another basin in the same region or a region with similar hydrological characteristics (Giannoni, Smith, Zhang, & Roth, 2003). The method plots the highest discharges recorded per unit area of the catchment against their corresponding areas in the region on a graph. Once plotted, the points derived from the graph are joined using an envelope curve (Chow et al., 1988). With the envelope curve, one can estimate probable maximum discharges of any basin within that region.

The equation to the envelope curve is;

$$q = C.A^{n}$$

Equation 2-15

Where; q - Peak flow per unit area, A-Catchment Area, C-constant, n-Index
to get the maximum peak flow, we multiply equation (2-15) above with the catchment area A and the resulting equation is represented as;

$$Q = C.A^{n+1}$$

Equation 2-16

Where Q is the maximum peak flow

2.3.3 The soil conservation service – curve number (SCS-CN) method

The soil conservation service – curve number (SCS-CN) method applies remote sensing together with GIS for rainfall-runoff modeling. The method has been tested and significantly applied for various watersheds in America (its origin), India, Europe, and in many other countries (Candela, Brigandì, & Aronica, 2014).

The method was developed in the United States of America by the US department of agriculture and soil conservation in 1972. Among the many existing rainfall-runoff analysis formula, the SCS – CN method is the most common. The method establishes a rainfall-runoff relationship of a basin and involves the application of simple equations together with readily available tables and curves.

For a rainfall event within a watershed, the direct runoff volume is less than or equal to the volume of the actual rainfall. Before runoff begins, the additional volume of water retained in the watershed F_a is less than or equal to the potential maximum retention of the soil S. Also, during the initial stages of the rainfall event, some rainfall amount I_a is abstracted even before any runoff occurs. The potential rainfall is '$P - I_a$ '(Mays, 2005)

The SCS-CN method is the most common, widely applied, and highly recommended by many researchers for discharge estimations (Xiao *et al.,* 2011). Hjelmfelt Jr, (1991) conducted a study using the SCS - CN procedure where he realized that the method is logically consistent and experimentally verifiable.

A review on the SCS-CN method conducted by Ponce and Hawkins (1996) established that the method has wide application in the United States and many other countries. The reasons being its advantage in the ease of use, stability, predictability, reliance on only one parameter, and its receptiveness to significant runoff generating properties (soil type, land-use, antecedent soil moisture, and landcover). However, just like many other procedures, Ponce and Hawkins (1996) pointed out the method`s significant setbacks. These included; its sensitivity to the CN, lack of clear guidance on how to vary the antecedent condition, and absence of clear guidance for the spatial scale effects as well as in determining the initial abstraction ratio.

Even though the basic theory of both the rational and the SCS-CN methods applies to large basins, their wide range of application is limited to areas less than or equal to 12 km^2 (Federal Ministry of Works, 2013). Areas bigger than this have storage and sub-surface flows, which results from runoff hydrograph attenuation and can lead to over-estimation of rates of flow using these methods. Larger basins of over 12km^2 require the application of an area correction factor (Federal Ministry of Works, 2013). The area correction factor is an approximation and does not factor the basin characteristics; thus, the application of both methods in larger basins needs careful consideration. If a correction factor is not applied, the basin can further be sub-divided into smaller sub-basins of

less than 12km^2 then peak flows from all the sub-basins combined together through hydrologic routing.

2.4 Urban flood risk management practices

2.4.1 Structural control measures

Structural flood control measures constitute one of the most conservative sets of interventions within a basin (Filho & Pina, 2010). Structural flood control measures have two categories; intensive and extensive. Intensive flood control measures refer to the modifications of the drainage channel such as; rectification and canalization, dike construction and dredging, and damping (Gomes & de Magalhaes, 2012).

On the other hand, extensive flood control measures are spread along the basin to control the runoff generation (Filho & Pina, 2010). The conservative drainage designs focused on the conveyance of the floodwaters within the basin. Modern methods focus more on storage and infiltration measures (Gomes & de Magalhaes, 2012). The following section describes some of the best structural flood management practices that have been applied successfully in similar basins.

a) Construction of detention basins

Detention basins are specifically designed to redistribute discharge over a long period a process known as flood damping (Filho & Pina, 2010). Detention basins minimize flood magnitudes but do not reduce the total runoff volumes since they hold water temporarily and later release volumes that do not lead to flooding. The damping process stores water after a rainfall event and regulates the volumes released through the use of limited discharge structures. There are different possibilities in which detention basins apply. They can be constructed across the drainage channel at the upstream, controlling a large part of the basin (Gomes & de Magalhaes, 2012). Detention basins require ample space and are best suited to places with less population. According to (Miguez, Mascarenhas, & Magalhães, 2005), public parks and squares together with riverine areas can serve as detention basins, which allows construction of multifunctional landscapes. Also, car packs when designed in a way that allows temporary storage of water can serve as detention basins (Filho & Pina, 2010).

Detention basins approach can significantly minimize flooding downstream. However, detention reservoirs need adequate spatial planning and adequately distributed to give a combined effect for overall flood risk mitigation (Gomes & de Magalhaes, 2012).

b) Development of retention ponds

Unlike detention basins, retention ponds are small scale permanent pools developed for two primary purposes; water quality control and water quantity control (Carlos Eduardo Morelli Tucci, 2007). Since retention ponds store water for a longer time, this allows the sediments in the water to settle, therefore minimizing the pollutants load of the water released.

c) Enhanced infiltration techniques

Urbanization means less of the green environment and more of the paved artificial environment. The whole process interferes with the natural hydrologic response of the catchment leading to quick runoff volumes generation a reason for the increasing urban flooding. Infiltration measures help to partly recover the natural hydrological behavior of the basin (WMO, 2008). The application of the infiltration measures might not be handy in highly populated areas. Based on how they function, infiltration measures have different groups namely; infiltration trenches, vegetated surfaces, Rain gardens, and permeable pavements (Gomes & de Magalhaes, 2012)

Infiltration trenches, which is one of the most common infiltration measures refer to linear excavations backfilled with gravel and stones. The trench is designed to store the diverted stormwater for a period that will sufficiently allow it to infiltrate into the soil (AMEC Earth and Environmenta, 2001). However, before the establishment of an infiltration trench, the soil must be well examined because different soils have different infiltration rates and in some soil groups, the method will not be efficient and can even lead to subsequent flooding from the diverted stormwater.

The vegetated surface is another approach that enhances the infiltration of stormwater. There are two types of vegetated surface, namely; filter strips and swales. Filter strips are highly recommended on regions with gentle slopes and are designed to enhance sheet flow (Butler & Davies, 2004; Webber et al., 2018). On the other hand, swales are shallow-grassed channels majorly for storage, infiltration, treatment, and conveyance of stormwater. These approach stores

water for infiltration with a drainage system designed in a way that the water will be conveyed back to the drainage channels once floods have receded.

Permeable pavement is another infiltration measure in which superficial stormwater flow infiltrates through a porous surface in a groundwater reservoir filled with gravel (Tschantz, Gangaware, & Morton, 2003). The upper layer of porous pavements is made up of open structured material (like concrete units) filled with small stones, gravel, and porous asphalt (Gomes & de Magalhaes, 2012). In some instances, the concrete structures are separated using grass. The effectiveness of this method is determined by filling the reservoir with porous material as well as the infiltration capacity of the soil. The method is greatly affected by clogging (Butler, Digman, Makropoulos, & Davies, 2018)

d) Canalization

Canalization is among conservative measures in the drainage works applied to urban flood management. It is the removal of obstructions from the riverbed as well as river course straightening and fixing its banks which eventually leads to enhanced transportation of the runoff volumes from the basin (Butler et al., 2018).

e) Dikes and polders

Applied as early as in the 12th century in the Netherlands, a polder refers to a low-lying piece of land forming an artificial hydrological unit enclosed by dikes. A polder can be reclaimed land, riparian area (floodplain) or marshes (Schoubroeck, 2010). The formation of a polder protects the area beyond the dike from flooding. The polder design allows temporary storage of floodwaters, and the dike has an auxiliary channel which conveys water from the polder area into the main channel. Flap gates or a pump to conveying the temporarily stored water once the levels drop is used (Schoubroeck, 2010)

2.4.2 Non-structural flood control measures

Structural measures act directly on the floods while non-structural flood control measures minimize the exposure or vulnerability of lives and property for flood risk. Several non-structural measures have been applied successfully applied to combat the flooding menace. The following section gives a review of some of the most common non-structural flood control measures.

a) The flood plain management

Non-structural flood control measures objective is to avoid or limit floodplain occupation. River or drainage channel overtopping is a natural phenomenon that has significant environmental relevance. As a result, it is, therefore, necessary to draft rules and regulations clearly defining the extent of the floodplain and what activities are allowed within the floodplain. In many urban areas, floodplain occupation is a serious problem. Floodplain usually presents unoccupied land and in instances where no flooding has been experienced for a long time, settling in these areas is very tempting. Moreover, the increased urban population also gives newbies little chance other than settling in risk areas especially in many developing countries where land-use control is not valid (Ashley, Garvin, Pasche, Vassilopoulos, & Zevenbergen, 2007).

The regulation and control of the floodplain must be guided by flood mapping to identify vulnerable areas to flooding and to recommend a land-use criterion. Most importantly, the approach must integrate with urban planning since urban master plans and zoning considers aspects linked to the management and regulation of floodplain (Gomes & de Magalhaes, 2012)

The flood plain can have two zones;

- The floodway which presents area subject to frequent flooding
- The flood fridge to represent area subject to flooding only from severe storms.

The realization of these zones is done through flood risk mapping using historical flood data. In many countries, the floodplain encroachment is illegal. Different countries have different regulations regarding the use of floodways (Butler et al., 2018). Quite often, the areas develop to public parks or environmental conservation zones. In some instances, occupation of the flood fridge is allowed but with set conditions. The government and public authorities can purchase or forcefully demolish structures constructed on flood risk areas. Demolition of structures on floodplains is typical, especially in many developing countries forcing the relocation of the affected people and properties (Gomes & de Magalhaes, 2012).

b) Flood management master plan (FMMP)

The flood management master plan constitutes measures, strategies, and policies put together to mitigate flood risk as well as guiding the development of the drainage networks. The development of a master plan factors in the whole basin. Besides, the plan must harmoniously integrate with all the other urban planning strategies, management instruments, regulations, and associated laws (Andjelkovic, 2001);

- Definition of goals and objectives based on future events
- Development of an inventory of all drainage networks and flood control infrastructures
- Gathering of hydrological data concerning rainfall, discharge measurements, and historical flood data
- A thorough analysis of flooding problems and the causes
- Flood risk mapping with land-use restrictions
- Proposal for applicable structural and non-structural flood control measures
- The design and estimations of costs for the proposed flood control measures
- Preforming the benefit-cost analysis for the proposed solutions as well as comparison with alternate solutions
- The definition of the design criteria of all drainage facilities
- Water pollution and soil erosion control techniques, among others.

c) Integrated Flood Management (IFM)

The Integrated Flood Management (IFM) applies policies, regulatory authorities, physical and financial measures in the wake of advancing from the conventional flood control measures to flood management that fully recognizes and appreciates holistic interaction between human habitation and the floods (WMO, 2015). IFM must address fundamental issues regarding sustainable development and the human's security from flood management viewpoint and within the Integrated Water Resources Management (IWRM) Framework (WMO, 2017a). Also, bearing in mind that the lower river reaches end up in the coastal area, the IFM framework must incorporate the Integrated Coastal Zone Management (ICZM). Flooding is a natural phenomenon which is closely related to the natural river system. Therefore, either structural and non-structural measures along the river channel or anywhere in the watershed will have a direct impact on the natural environment which can lead to environmental degradation thus limiting the natural ecosystem services (WMO,

2007). An effective and efficient urban flood management strategy has to focus on its integration into the already existing IWRM. The integration of the IFM and IWRM ensures the capturing of the economies of scale, thus creating collaborations where possible to avoid any maladaptive behavior (WMO, 2017b).

When taking the decisions regarding what action to take to address floods within a city, the process involves consideration of several factors. Any action undertaken in the upper reaches of the watershed has dire effects on the lower reaches of the same watershed. Some can amplify the flood generation, and others can decrease significantly the amount of water reaching downstream, thus interfering with the water quality too. Efforts directed towards keeping floodwaters away from the urban area may significantly affect the sub-urban populations or other nearby agricultural and industrial areas positively or negatively.

The land-Use planning, Zoning, and Development arrangements need to be critically analyzed and implemented in a way that will ensure maximum benefit for the whole watershed (WMO, 2017b). However, these strategies must gear towards the protection, and the enhancement of the environmental quality, as well as the ecosystems services flow (WMO, 2007).

d) Real-Time Flood Forecasting

With future projections depicting the increase of extreme events, real-time flood forecasting, remains one of the most reliable tools towards flood risk management. Despite the systems of nature being dynamic and unpredictive, specific indicators send signals of the magnitude of the forthcoming event. These indicators help planners and decision-makers as well as emergency response units on what preparatory measures have to be put in place to minimize the impact of the phenomenon once it strikes. An efficient real-time flood forecasting system has been applied in many places of the world and has saved significant amounts of property and lives against damage. Flood forecasting largely relies on historical data and models; that is a reliable data collection and communication system as well as an approximating methodology (Carlos E. M. Tucci, 2007). These systems are used in the transmission of precipitation, gauge level, and discharge data as an event occurs. Once the data is received, projections are simulated using mathematical models that represent the nature of various water cycle phases.

Flooding magnitude can be forecasted based on the precipitation data, precipitation forecast, upstream discharge or based on both the precipitation and the upstream discharge. The first step involves the projection of the precipitation likely to fall within the watershed (done using remote sensing or radar technology) to perform a flood forecast based on precipitation forecast. Once the precipitation data for the watershed after obtaining the precipitation data of the basin, the next step is runoff simulation through the application of models that convert precipitation into discharges.

e) Urban flood management strategies

The urban flood management strategies, plans, and approaches all have standard features. They mainly focus on the technical, i.e., Engineering and Hydraulic designs aspects of flood management. They do not consider the very fundamental and real ecological, environmental, socio-economic, and political aspects for flood management. According to Tucci (2007), "Flooding is controlled by a combination of structural and non-structural measures enabling the vulnerable population to minimize it loses and continue to live in harmony with the river. These include all the aspects - engineering, social, economic, and administrative measures. Planning of protection against flooding and its effect involves research into an ideal combination of these measures".

The management of urban floods should deal explicitly and directly with the drinking water supply, stormwater disposal, sewage, and wastewater disposal while managing both the stormwater quantity and its effect on the water quality (WMO, 2017b). Also, the responsible authority for urban flood management needs to adopt the integrated flood management framework to realize the more significant issues of efficiency, effectiveness, socio-economy equity, and all other long-term outcomes.

Flood risk management has various goals based on numerous time and space scales. Achieving these goals depends on both the development and implementation of suitable portfolios of measure, a procedure marred by the complicated nature of the flooding system. Flood risk management embeds a gradual adaptation process different from the "implement and maintains" philosophy of the conventional flood control ensures (Sayers et al., 2013). A strategic flood risk management factors in the whole system and gives priority to the most vulnerable populations. It comprises a concerted effort across all government stakeholders, businesses, the public sector, non-governmental organizations, and individuals.

CHAPTER THREE

3 DESCRIPTION OF THE STUDY AREA

3.1 Location

Niamey is the capital and the largest city of Niger. The city has a population of about 1,302,910 people. Study area bound by longitude $2^0$2'30" E and $2^0$7'30" E and Latitude $13^0$30'0" N and $13^0$35'0" N. A weak slope generally characterizes the basin, with elevation varying between 160 m above sea level to 250 m above sea level. The city serves as an administrative, social and economic center for Niger.

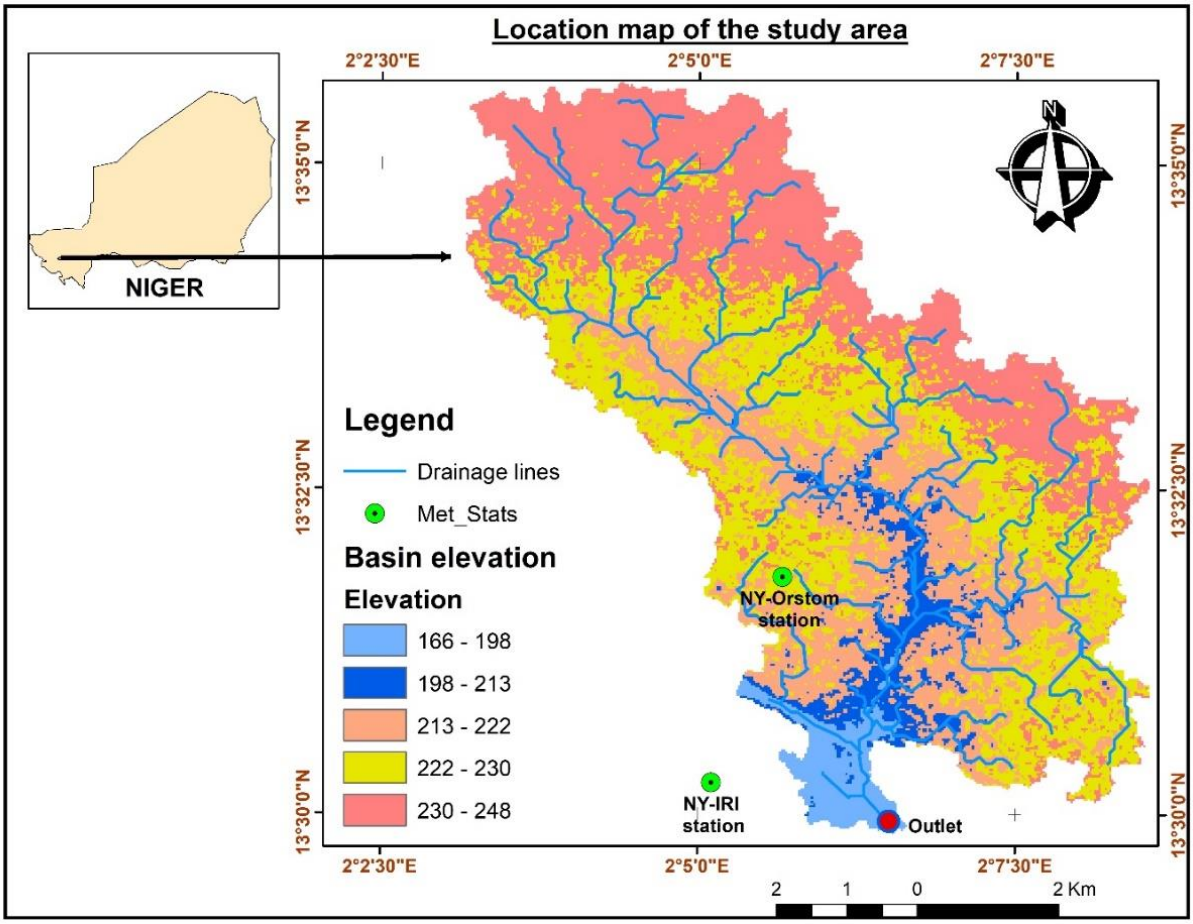

Figure 3: The location of the Gountiyena basin, Niamey-Niger

3.2 Weather

The Niamey weather is arid with an annual average temperature of 30^0 C. Niamey experiences average minimum temperatures during December and January. In April, which is also known as

the hottest month the temperatures go as high as 45^0 C. The city receives an annual average rainfall of about 500 mm during the rainy season spread from May to August.

3.3 Hydrology of the study area

River Niger is the largest river that cuts through the city. Initially, the city was on the left bank of the river, however, with recent developments and urbanizations, the city now lies on both banks of the river Niger which is the largest river in the country and the Third Largest River in Africa after River Nile and Congo based on the area of coverage. The city has other seasonal small rivers and tributaries located on the left side of the Niger River. These tributaries and small seasonal rivers build up very fast when it rains and are responsible for the flooding menace affecting Niamey city.

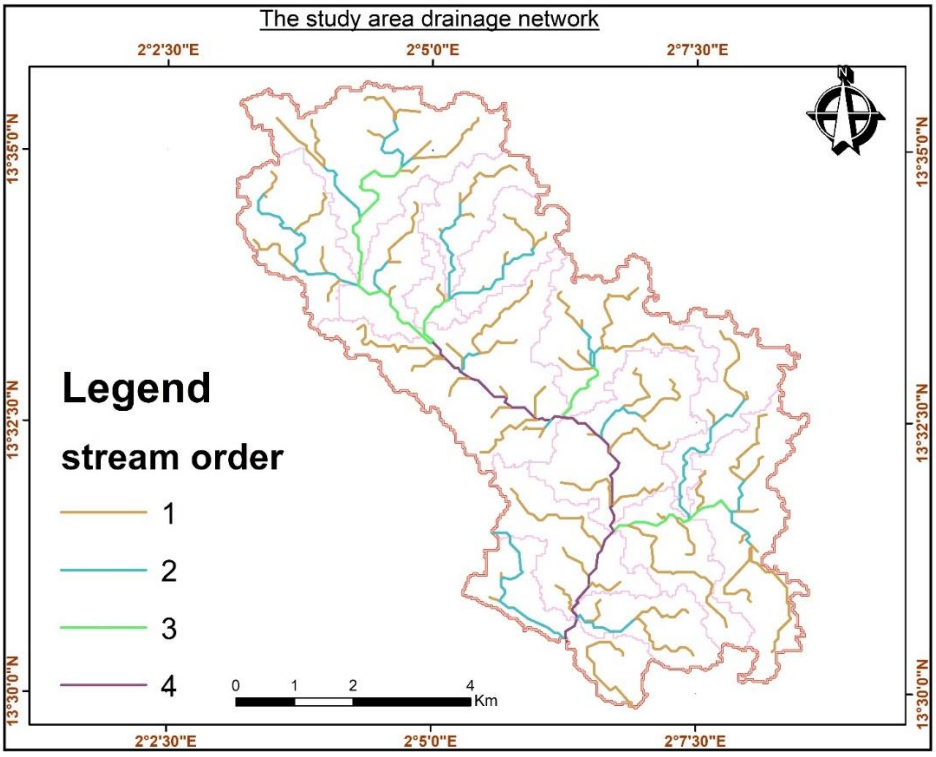

Figure 4: Drainage network of the study area

3.4 Geological setting of the study area

The geology of Niamey city lies between the West Africa Precambrian Craton and formations belonging to the sedimentary basin of the Iullemmeden referred to as the Paleo-Mesozoic and Tertiary Covers. The city lies on a bedrock composed of the Precambrian intrusive rocks (diorites and the Granites) and Micaschist with intrusions of Quarzitic. The rock near the surface are generally the Continental Terminal (CT) of the Pliocene age, and they represent the upper end of

the sedimentary deposits of the Iullemmeden basin sandstones and sandy clay. The continental terminals have quaternary deposits made up of armor ferruginous laterites formed after the tertiary through colluvial deposits, dunes, terraces, and alluvial sediments (Lasagna et al., 2015). The laterites and the alluvial sediments have attracted quarrying activities. Alluvial sediments produce sand and gravel for building activities, and the laterites serve as quarries for road construction works.

The hydrogeology of Niamey city is composed of two shallow aquifers of different permeabilities. The first one located at the center of the city on the left bank of Niger river is on the base of the transformed Precambrian bedrock, and its permeability linked to cracks. The second aquifer positioned on both the banks of the Niger River in deposits of the Continental Terminal and the recent alluvial deposits and its permeability attributed to porosity. These aquifers are recharged through indirect infiltration from surface water, i.e., ponds and from direct infiltration, i.e., sand-dunes (Lasagna et al., 2015).

3.5 Data collection

The data applied in this research include historical rainfall data, digital elevation model (DEM), Land-use Landcover (LULC), and soil data.

3.5.1 Digital elevation model (DEM)

The Digital Elevation Model used in this research is from the Shuttle Radar Topography Mission (SRTM) website. The downloaded DEM had a spatial resolution of 30m by 30m. The DEM is instrumental in watershed model delineation since it describes the catchment terrain. It was processed in ArcGIS using the Arc Hydro tools to generate drainage channels, watershed boundary, and slope. Stream order was generated using spatial analysis tools.

3.5.2 Climate Data

For this study, a 5-minute rainfall data from the year 1990 to 2017 is from the AMMA Observatory Center in Niamey for both NY-IRI and NY-ORSTOM Rainfall Stations. From the observed data, the annual maximum for different durations was extracted. Two stations were considered for the development of the IDF curves for the study area as well as for the peak discharge estimations.

3.5.3 Combined Land-use Landcover and hydrologic soil groups data

The current study applies the combined land use- land cover and hydrologic soil group. The data is from the WASCAL Competence center, Ouagadougou Burkina Faso Department of remote

sensing. The soil data were downloaded from the ORNL DAAC website with the name Global Hydrologic Soil Groups (HYSOGs250m) for Curve Number-Based Runoff Modelling.

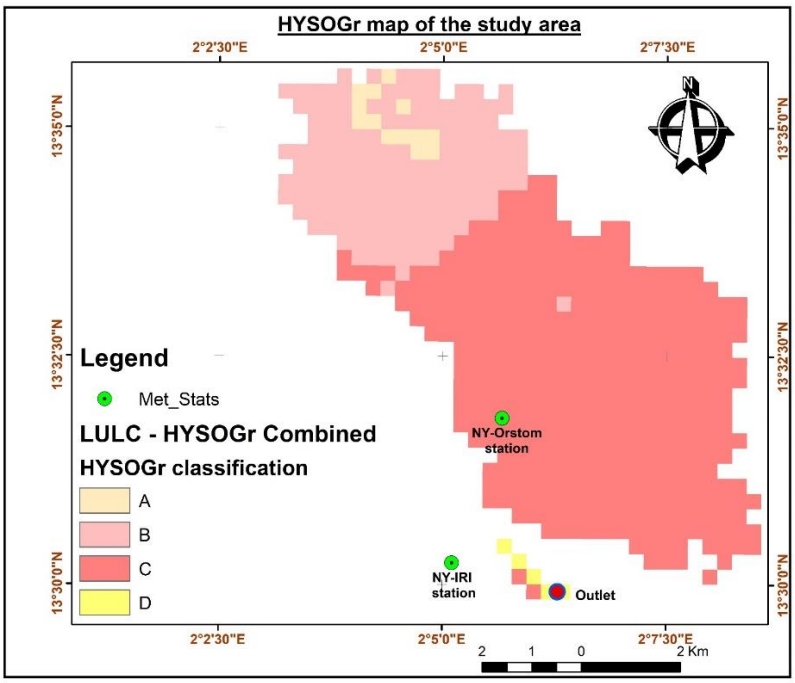

Figure 5: HYSOGr map of the study area

The land-use land-cover map for the study area given in figure (6) below. From the figure, the built-up area covers more than half the basin. The upper part of the basin, which represents the upstream is less developed with majorly vegetation and bare soil.

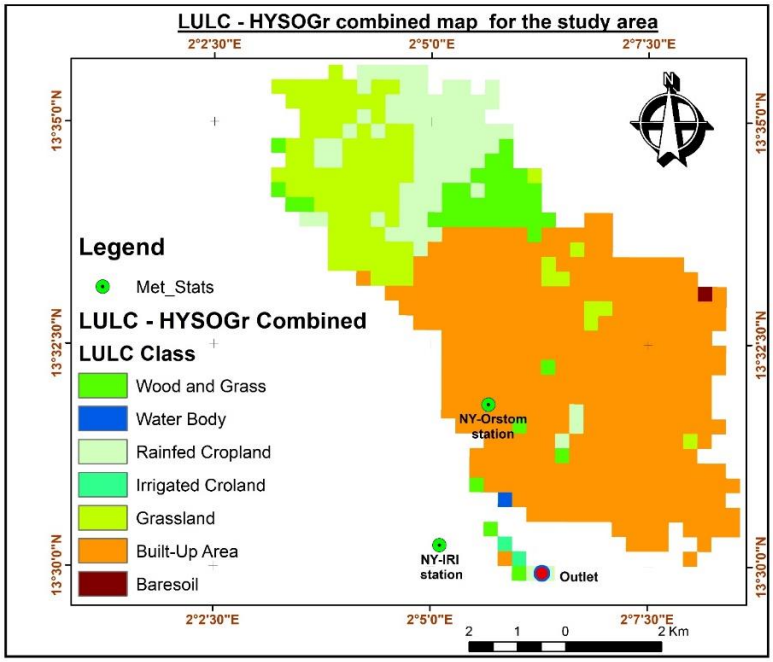

Figure 6: LULC - HYSOGr combined map for the study area

Figure (7) is the slope map classified into three classes; low, medium, and high. About two-thirds of the study area has a slope of less than 13%, and the average slope for the whole study area is 5.8%.

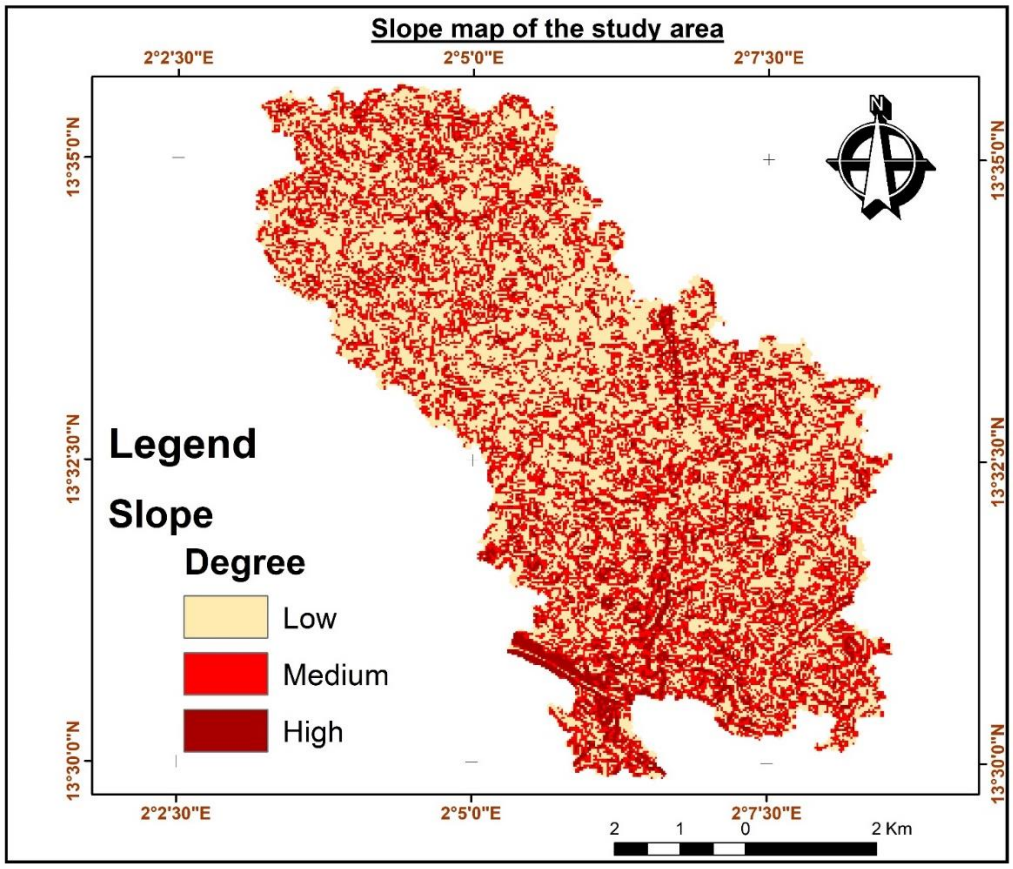

Figure 7: slope map for the study area

Other useful parameters and basin characteristics for the application of the Rational method were computed using both ArcGIS toolbox and in excel. Table (18) below gives the obtained results.

CHAPTER FOUR

4 METHODOLOGY

The methodology develops around the specific objectives of the work. The process for selecting the appropriate probability distribution function for IDF analysis, the peak discharge estimation methods for the present ungauged basin, and the method for identifying appropriate flood management options for the study area are described in the following lines.

4.1 Selection of the Appropriate probability distribution function

The current study applies the Gumbel and the Log Pearson Type III (LPT III) distributions the most appropriate distributions for the development of the Intensity Duration Frequency (IDF) (See for instance Koutsoyiannis et al., 1998; and Oyebande, 1982). The following procedure was followed to identify the most appropriate distribution between the two;

1) The fitting of the Annual Maximum Series (AMS) for every duration for both the Gumbel and the LPT III Distributions through the application of the EasyFit Software (MathWave Technologies, 2019).

2) The Chi-square and the Kolmogorov Smirnov Tests of goodness-of-fit at a significance level of 5% were applied for each rainfall duration to determine which distribution fitted well to the data.

3) The distributions were then ranked based on the goodness of fit. The rank 1 refers to the distribution indicating the best fit and ranks two the distribution with the less acceptable fit.

4) The Gumbel distribution provided a better fit as compared to the LPT III distribution with seven (7) out of nine (9) durations having a rank of one. The frequency analysis in this study applied the Gumbel distribution.

4.1.1 Fitting the Gumbel distribution to sample data procedure

The main objective of fitting a sample data to a statistical distribution is to help in determining the distribution parameters of the sample data as well as verifying whether the sample comes from the statistic. The Gumbel Distribution fitted well to our data, and the following steps describe the fitting procedure. After fitting the sample, the goodness-of-fit test will be performed to evaluate the fitting validity. After fitting the sample into the distribution, the next step includes the

estimation of the low or high probability of occurrence events from the distribution. The fitting procedure includes the following steps;

1. The first step is the ranking of the annual maximum series values of the observed data in descending order from the highest to the lowest, then applying a rank *m* to each event. Rank *m* = 1 represents the highest value, and the lowest value is given a rank *n (n is being the sample size)*.
2. The computation of the exceedance probability. Several methods can be applied, such as; the Gringorten formula and the Weibull formula in estimating the cumulative probability distribution to compute the probability of exceedance. Between the two methods, the Weibull formula is asymptotically exact only for a population with primary uniform distribution, a phenomenon that is naturally rare (Maidment, 1996). The Gringorten formula is recommended to tackle this drawback, and the probability of exceedance was estimated using the equation (4-1) given below;

$$p = \frac{m - 0.44}{N + 0.12}$$

Equation 4-1

For values of $p = p(X \geq x)$; and $p = 1 - F(x)$ and $f(x) = p(X < x)$

3. The computation of the reduced variable *p* using equation (4-2) given below;

$$u = -\ln[-\ln(1 - p)]$$

Equation 4-2

4. After computing the reduced variable μ, the sample average μ_s is computed together with the standard deviation σ_s.
5. The χ_0 and s parameters of the Gumbel distribution were computed using equation (4-3) below;

$$x_0 = \mu_s - \frac{\mu_N}{\sigma_N}\sigma_s$$

Equation 4-3

μ_N is the average of the reduced variable

$$s = \frac{\sigma_s}{\sigma_N}$$

Equation 4-4

Where σ_N – the reduced variable standard deviation

6. The sixth step involves the computation of the Gumbel mean (μ_G) and the standard deviation (σ_G) using equations 4-5 and 4-6 respectively

$$\mu_G = x_0 + 0.5772\ X\ s$$

Equation 4-5

$$\boldsymbol{\sigma_G = 1.2825\ X\ s}$$

Equation 4-6

For all the ranked values, the Gumbel variable is usually obtained using equation (4-7) given below;

$$x_G = x_0 + u\ X\ s$$

Equation 4-7

The variables obtained are used to compute the desired data.

4.1.2 The Gumbel distribution frequency factor

After fitting the distribution into the data sample, all the extreme (X_T) values relating to a specific return period larger than or equal to 2-years were calculated using the following formula (Chow et al., 1988)-:

$$X_T = \mu_G + K_T\ X\ \sigma_G$$

Equation 4-8

Where; μ_G - Gumbel Mean, σ_G - Standard Deviation and K_T- Coefficient Factor based on the return period T given by;

$$K_T = -\frac{\sqrt{6}}{\pi}\{0.5772 + \ln(\ln(\frac{T}{T-1}))\}$$

Equation 4-9

In the case where T < 2,

$$K_T = -\frac{\sqrt{6}}{\pi} X \left[0.5772 - \ln T + \frac{1}{2\,X\,T} + \frac{1}{24\,X\,T^2} + \frac{1}{8\,X\,T^2}\right]$$

Equation 4-10

4.1.3 The Goodness of fit test

The two widely applied goodness-of-fit methods in hydrology; i.e., the Kolmogorov-Smirnov and the Chi-Square methods were applied (Machiwal & Jha, 2012).

a) The Kolmogorov-Smirnov test

The Kolmogorov-Smirnov test procedure for the goodness of fit tests is as follows;

i. The cumulative sample distribution expressed as a function $f_0(x)$based on N observations. For every observed (*x) value*, then $f_0(x) = \frac{j}{N}$, where *j* is the number of observations which are less than or equal to *x*.

ii. The reduced variable (u) is computed using the expression

$$u = \frac{X_0 - x_0}{s}$$

where; X_0 - sample value, x_0 - position parameter and s - scale parameter

iii. The cumulative distribution function in the null hypothesis is a function $f_t(x)$. Gumbel Cumulative probability distribution triggers theoretical cumulated probabilities expressed as;

$$f_t(x) = f(u) = e^{-e^{-u}}$$

Equation 4-11

iv. Finally, the maximum deviation *D* is determined using the equation (53) below;

$$D = \max[f_o(x) - f_t(x)]$$

Equation 4-12

b) The Chi-Square tests

The chi-square goodness-of-fit test is as below;

i. The observed data (O) and the expected data (E) are classified into intervals to determine their frequencies in each class. The results of this can be well presented using a histogram

ii. The classifications are rearranged to make the minimum expected frequencies in each class of five or higher (low-frequencies classes merged).

iii. The chi-square values for the intervals using equation (4-13) below are determined

$$x^2(v) = \sum_i^n \frac{(O_i - E_i)^2}{E_i}$$

Equation 4-13

Where; *v* - degree of freedom and is given by *(n-k-1)*, *n* - number of intervals and *k* - number of distributions parameters obtained

Both n and k are constraints presumed to the fitting process.

iv. The chi-square value obtained is then compared to the $x^2{}_{0.05}$ from chi-square tables. The null hypothesis is accepted if;

$$x^2 < x^2{}_{0.05}$$

Equation 4-14

So, rejected if otherwise.

4.2 Peak Discharge Estimation

4.2.1 The Rational Method

The peak discharge is computed using the following equation (4-15) below (Chow et al., 1988);

$$Q = C_u C i A$$

Equation 4-15

Where; Q - peak discharge (m^3/s), A - basin Area (hectares), C_u - units conversion (dimensionless), C - runoff coefficient (dimensionless), i - design rainfall intensity (mm/hr)

The unit's converter C_u is key because the iA product regardless of having units of L^3/T does not serve as standard units based on the conventional unit's system.

The following procedure was applied to compute peak discharge using the Rational method;

1. Determination of the drainage area in hectares

The area reduction factor f_A was estimated using equation (4-16) to avoid over-estimation of the discharge computed (Federal Ministry of Works, 2013).

$$f_A = \frac{1}{e^{\left(1-\frac{12}{A}\right)}}$$

Equation 4-16

The corrected area was computed using equation 4-17 below.

$$A_{corrected} = A - (f_A X\ A)$$

Equation 4-17

2. Determination of the runoff coefficient (Table 18)

A basin with a homogenous land-use and soil-cover applies runoff coefficient directly from the runoff coefficient table (Chow et al., 1988). Heterogenous basins with different land use and soil cover require further considerations before choosing the runoff coefficient. The area must be sub-divided into different sub-areas of homogeneous characteristics. The surface area of each sub-are is calculated together with its corresponding runoff-coefficient (C). The average, weighted runoff-coefficient value is calculated using equation (4-18);

$$C_w = \frac{\sum_{j=1}^{n} C_j A_j}{\sum_{j=1}^{n} A_j}$$

Equation 4-18

Where; A_j - homogeneous land cover and soil type area, C_j - runoff coefficient for the corresponding homogeneous landcover/soil type, n - number of distinct land cover/soil type in the watershed and C_w - weighted runoff coefficient

The classification of the basin into different sections considers the slope, Land-Use-Land-Cover (LULC), and the soil type. Different LULC, soil type, and varying slope have a direct impact on

the runoff generation. A loose soil like sandy soil in a low-lying area will produce insignificant runoff as compared to tight soils such as clay on a steep slope.

Sandy soils have higher infiltration rates leading to relatively low runoff generation and consequently low runoff coefficient. On the other hand, soils with minimal infiltration rate (clay soil) have relatively high runoff rates and high runoff coefficient as well.

According to the United States Soil Conservation Service (SCS), there are four classifications of hydrologic soil groups (A, B, C, and D) that are fundamental for the runoff coefficient determination. The soil group identification is done through the assessment of the soil`s infiltration capacity or based on its characteristics. The different infiltration rates for different SCS soil groups are as follows (McCuen, 1998);

Table 1: Description of the four SCS different soil groups

Group	Infiltration rate (inches/hr)	Soil texture
A	0.30 – 0.45	Deep Sand, Deep Loess, Aggregated soils
B	0.15 – 0.30	Shallow Loess, Sandy Loam
C	0.05 – 0.15	Clay Loams, Shallow Sandy Loam, low organic matter, high clay soils
D	0.00 – 0.05	Swell significantly when wet, heavy plastic soils, specific saline soils

3. Determination of the longest flow path length of the basin

In the application of the Rational Method, the determination of the longest flow path in the basin is a must. To be able to determine the time of concentration, which then helps in determining the time to peak, we must first compute the length of the longest flow path. The determination of the longest flow path was through ArcGIS, where the longest flow path of each sub-basin was computed and then summed up together to get the longest flow path.

4. Time of Concentration and Peak Time

The time of concentration is equivalent to the summation of the travel times for all the flow regimes. It is the total time required by a volume of water to travel from the most remote point of the basin to the basin outlet. To be able to compute the peak discharge using the Rational Method, the Time of concentration T_c is essential. The time of concentration will also help in computing

the duration of excess flow, time lag, and the time to peak used in the computation of the rainfall intensity for peak discharge estimation.

The time of concentration was computed using the Kirpich Formula equation (4-19)

$$t_c = 0.0195\left(\frac{L}{\sqrt{s}}\right)^{0.77}$$

Equation 4-19

Where; t_c - Time of concentration in minutes, L - The length of the longest flow path in meters and S - the average slope of the basin in m/m

from the time of concentration, the time lag can be determined using the relationship established by the United States department of agriculture soil conservation service (SCS). The SCS established that the time lag is 0.6 percent of the time of concentration equation (4-20) below;

$$T_{lag} = 0.6t_c$$

Equation 4-20

Where; T_{lag} - Time lag and t_c –Time of concentration

During a precipitation event, once all the storages are satisfied, runoff starts. The duration of the excess rainfall will be computed using the relationship equation (4-21)

$$D = 0.133t_c$$

Equation 4-21

Where; D – Duration, and t_c – the time of concentration

The US department of agriculture soil conservation service further established the relationship between duration of excess rainfall, time of concentration, and peak time. The following equation (4-22) will be applied to calculate the time to peak

$$T_p = \frac{D}{2} + 0.6t_c$$

Equation 4-22

Where; T_p – time to peak, D– duration of excess rainfall, and t_c – a time of concentration

5. Rainfall intensity

Rainfall intensity for the design of engineering structure designs depends on;

i. Return period
ii. The characteristics of the intensity duration of the selected rainfall return period
iii. The time of concentration of the watershed

The rainfall intensity can be determined using different approaches such as;

i. The intensity duration frequency equation
ii. The established IDF curves

The current study applied the IDF curves in determining the rainfall intensity for different return periods to estimate peak discharges using the rational method.

6. Peak discharge estimation

The peak time will help in calculating the rainfall intensity in that specific time for use in the rational method for discharge computations. After all the parameters for the Rational method are established, the formula is then applied to calculate peak discharge for different intensities of different return periods.

$$Q = C_u CiA$$

The peak time helps in calculating the rainfall intensity since peak discharge comes during the peak rainfall.

Rainfall intensities for different return periods were calculated using the following relationship for the estimations of peak discharges for the same period

$$X_T = \mu_G + K_T \, X \, \sigma_G$$

Where; μ_G -Gumbel Mean, σ_G - Standard Deviation, and K_T -Coefficient Factor based on the return period

4.2.2 The SCS-CN Method

The SCS-CN method was applied in this study to estimate peak runoff for the catchment. The method applies daily annual maximum rainfall values. The runoff depth Q (mm) was estimated using equation (4-23) while the initial abstraction I_a using equation (4-24).

$$Q = \frac{(P - I_a)}{\{(P - I_a) + S\}}$$

Equation 4-23

Where;

Q – Peak discharge (mm), P – daily annual maximum rainfall depth, I_a – Initial abstraction and S – storage

This equation is only applicable for P greater than or equal to the initial abstraction otherwise no discharge

$$I_a = 0.2S$$

Equation 4-24

The storage S was computed using equation (4-25) below

$$s = \frac{25400}{CN} - 254$$

Equation 4-25

The Curve number was generated using ArcGIS tools. Since the basin is not homogeneous, a weighted CN was calculated using the hydrologic soil group map, land use land cover and the antecedent soil moisture for the study area.

Table 2: Classification of Hydrological Soil Groups

Group	Infiltration rate (mm/hr)	Soil Texture
A	high >25	Deep sand, deep loess, aggregated silt
B	moderate 12.5 – 25	Shallow loess, sandy loam
C	low 2.5 – 12.5	Clay Loams, shallow sandy loam, soils low in organic content, and soils usually high in clay
D	very low <2.5	Soils that swell significantly when wet, heavy plastic clays, and certain saline soils

The Weighted CN for the basin was calculated based on the soil classes as well as their corresponding hydrologic soil group and CN values.

It was calculated using the following equation (4-26)

$$CN = \frac{\sum_{j=1}^{n} A_j CN_j}{\sum_{j=1}^{n} A_j}$$

Equation 4-26

Where; A_j – the area of the specific soil class j, and CN_j – curve number for the hydrologic soil group and corresponding soil class.

To determine the daily peak runoff Q_p, the Brouwer 1997 method equation (4-27) below was applied

$$Q_p = 2.8 \frac{Q\ X\ A}{T_p}$$

Equation 4-27

Where; Q_p – peak runoff rate in m^3/s, Q – the storm runoff or volume of excess rainfall in mm, A – area of the basin, and T_p – time to peak in hrs.

Time of Concentration and Peak Time was computed using the same procedure in section (4.2.1)

The SCS-CN Method gives good results for small catchments. The area reduction factor f_A was estimated using the following equation to avoid over-estimation of the discharge computed (Federal Ministry of Works, 2013).

$$f_A = \frac{1}{e^{\left(1-\frac{12}{A}\right)}}$$

$$A_{corrected} = A - (f_A * A)$$

The corrected area applies for the discharge computation in place of the original area.

4.3 Flood risk management practices

Existing literature depicts that urban flooding is a global issue, and its severity is increasing annually. Concerning future climate projections, the frequency of precipitation events of even higher magnitudes is certain. It is due to these reasons that an efficient flood risk management plan is necessary. The quality of the available data determines the development of a comprehensive, competent, and appropriate flood risk management strategy. On the contrary, many urban basins are ungauged, but yet the most affected or are most likely to be severely affected by these increasing flooding event. It is therefore essential to utilize the available data in simulating useful information for the design, development, and implementation of flood risk management strategies exhaustively.

The Gountiyena basin is ungauged with no recorded discharge and flood data. The current research analyzed the basin through the application of remote sensing and rainfall data available. The obtained results helped to suggest appropriate flood management options for application within and beyond the Gountiyena basin. Some of the suggestions came from the successful application of the methods in other similar basins. With flooding in cities happening in both developed and developing countries, the study included a comprehensive literature review on the best flood management options. Finally, the study selected the most efficient and applicable flood management options out of the many reviewed measures.

CHAPTER FIVE

5 RESULTS AND DISCUSSIONS

This section presents the result obtained after applying the different procedures explained in the methodology. The results are in three parts; the intensity duration frequency analysis, the peak discharge estimations, and the recommendation of the best flood management practices for the study area.

5.1 Intensity Duration Frequency Analysis

5.1.1 The probability selection process for different rainfall durations

After fitting the two selected goodness-of-fit tests (Kolmogorov-Simonov and Chi-Square tests) to both distributions (Gumbel and LPT III) for all the duration, the results in the table (3).

It emerged that the Gumbel distribution fitted better as compared to the Log Pearson Type III Distribution. The comparison of the two distributions compared applied rank 1 to the best distribution. For the five minutes duration, the Gumbel distribution performed well than the LPT III (table 4).

Table 3: Summary of the Goodness-of-fit test for the five minutes (0.08 hrs) duration

Distribution	Kolmogorov-Smirnov		Chi-Squared	
	Statistic	***Rank***	***Statistic***	***Rank***
Gen. Extreme Value	0.12412	1	0.89661	2
Log-Pearson Type III	0.12699	2	0.78563	1

All other durations fitted for both rainfall stations (NY-IRI and NY-ORSTOM) given in table 4. It emerged that, out of the selected nine durations, Gumbel ranked well as compared to the LPT III for the two tests performed (Table 4).

Table 4: Gumbel and the Log-Pearson Type III Distribution Ranking

	NY-IRI Station				NY-ORSTOM Station			
	Kolmogorov		Chi-Square		Kolmogorov		Chi-Square	
Duration hrs	**Gum**	**LPT III**	**Gum**	**LPT III**	**Gum**	**LPT III**	**Gum**	**LPT III**
0.08	1	2	2	1	2	1	2	1
0.17	1	2	1	2	1	2	1	2
0.25	2	1	1	2	1	2	2	1
0.5	2	1	2	1	2	1	2	1
1	1	2	1	2	2	1	1	2
2	1	2	2	1	1	2	1	2
6	1	2	1	2	2	1	1	2
12	1	2	1	2	1	2	2	1
24	1	2	2	1	1	2	2	1

5.1.2 The annual-maxima series analysis

Table 5gives the parameters of the annual maxima series for different durations. The reduced variable average $\boldsymbol{\mu_N}$ for different durations was computed together with the standard deviation of the reduced variable $\boldsymbol{\sigma_N}$. The sample mean varies between 10.75 and 61.34 mm with a corresponding standard deviation between 2.83 and 26.66. The average rainfall values increase with the increasing rainfall duration.

Table 5: Annual-Maxima Series Distribution Parameters for the NY-IRI station

Parameters	**0.08 hrs**	**0.17 hrs**	**0.25 hrs**	**0.5 hrs**	**1 hr**	**2 hrs**	**6 hrs**	**12 hrs**	**24 hrs**
Sample Mean ($\boldsymbol{\mu_s}$)	10.75	19.07	25.26	36.45	45.25	51.43	58.51	60.24	61.34
Sample S.dv ($\boldsymbol{\sigma_s}$)	2.83	4.38	5.95	8.82	13.46	21.74	25.22	25.88	26.66
Post Parameter ($\boldsymbol{x_0}$)	**9.46**	**17.07**	**22.55**	**32.43**	**39.11**	**41.52**	**47.01**	**48.43**	**49.18**
Scale Parameter ($\boldsymbol{s}$)	**2.30**	**3.55**	**4.83**	**7.16**	**10.92**	**17.63**	**20.46**	**21.00**	**21.62**
Gumbel Mean ($\boldsymbol{\mu_G}$)	10.78	19.12	25.34	36.56	45.41	51.70	58.82	60.56	61.66
Gumbel S. dv ($\boldsymbol{\sigma_G}$)	2.94	4.55	6.19	9.18	14.00	22.62	26.24	26.93	27.73
Mean Red var ($\boldsymbol{\mu_N}$)	0.56	0.56	0.56	0.56	0.56	0.56	0.56	0.56	0.56
S. dv red var ($\boldsymbol{\sigma_N}$)	1.23	1.23	1.23	1.23	1.23	1.23	1.23	1.23	1.23

If the distribution parameters obtained are acceptable, they can then help in computing annual-maxima values for periods beyond the sample population period. The five minutes duration was applied to test both the scale and the position parameters for the sample population, and both the observed sample and the estimated values were compared (table 6).

The annual maximum series distribution parameters together with the observed and the expected annual maxima values for NY-ORSTOM station are in tables (26 & 27) appendix (B)

Table 6: The 0.08 hrs observed and expected Annual-Maxima values (NY-IRI Station)

Year	Rank (m)	5 Min (X_0)	P	U	X_G
1995	1	18.53	0.019915	3.906259	18.43
2005	2	17.42	0.055477	2.863394	16.03
2000	3	14.27	0.091038	2.349127	14.85
2010	4	13.24	0.1266	1.999803	14.05
2002	5	13.14	0.162162	1.731997	13.43
2017	6	11.84	0.197724	1.512753	12.93
1997	7	11.75	0.233286	1.325608	12.50
1998	8	11.7	0.268848	1.161125	12.12
1994	9	11.49	0.30441	1.013368	11.78
2008	10	11.2	0.339972	0.878339	11.47
1993	11	11.08	0.375533	0.7532	11.19
2016	12	11.07	0.411095	0.635839	10.92
1990	13	11.06	0.446657	0.524624	10.66
1992	14	11.03	0.482219	0.418242	10.42
2012	15	10.55	0.517781	0.315592	10.18
2003	16	10.3	0.553343	0.215716	9.95
2004	17	10.23	0.588905	0.117737	9.73
2009	18	10.23	0.624467	0.020807	9.50
1999	19	9.42	0.660028	-0.07594	9.28
2006	20	9.21	0.69559	-0.17343	9.06
1996	21	9.04	0.731152	-0.27278	8.83
2001	22	8.93	0.766714	-0.37534	8.59

1991	23	8.55	0.802276	-0.48297	8.35
2007	24	7.75	0.837838	-0.59837	8.08
2011	25	7.45	0.8734	-0.72596	7.79
2014	26	7.1	0.908962	-0.874	7.45
2013	27	6.88	0.944523	-1.06188	7.02
2015	28	6.44	0.980085	-1.36515	6.32

The estimated values ($\mathbf{X_G}$) computed through the application of the distribution parameters. A good example is table (6) for the five minutes duration where the distribution parameters were applied to compute the expected annual maxima values for the whole observation period 1990 to 2017. The results obtained for the estimated annual maximum values using the distribution parameters (scale and position parameters) was a good indicator that the obtained parameters were acceptable. Table (6) also presents the exceedance probability for the five minutes duration for the period 1990 to 2017, which was computed using the Gringorten method.

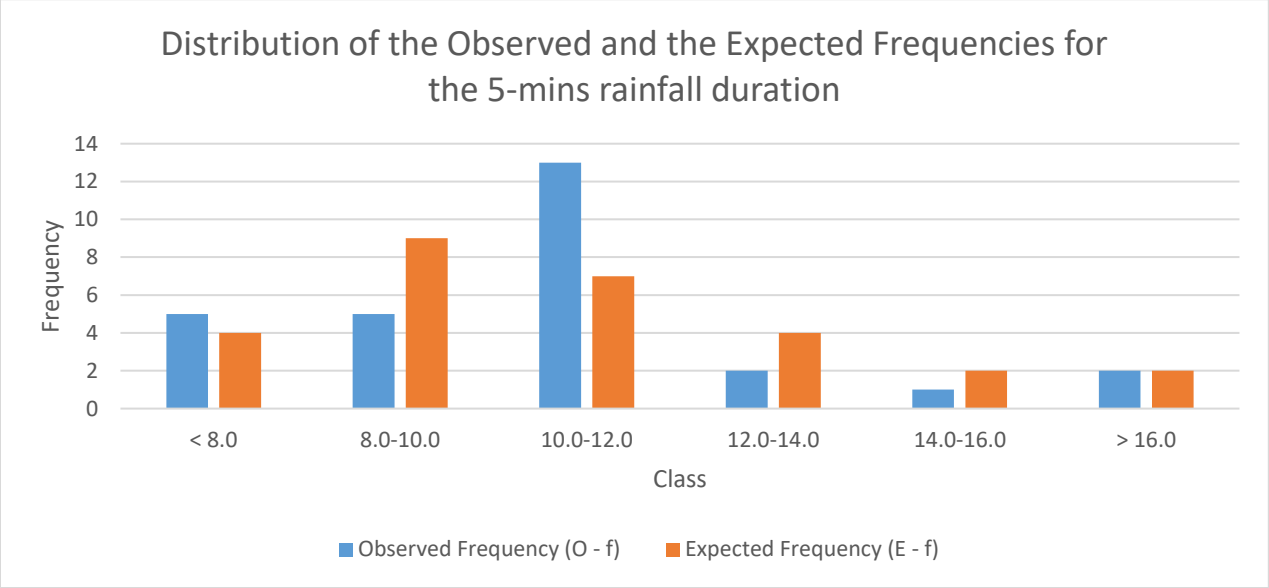

Figure 8: Distribution of the Observed and the Expected Frequencies

Figure (5) gives a comparison of how the observed and the estimated values vary. The observed data gives a high frequency for the events between 10 – 12 mm while the estimated values indicate a high frequency for events between 8 – 10 mm. However, both results produce a low frequency for events of higher magnitude. From both the observed and the estimated values, we can have a

good understanding of how the data will behave once fitted to a distribution. From the histogram, figure (5), it is clear that the statistic might skew and we can conclude that the distribution tails towards the right.

The close correlation between the observed and the estimated annual maximum values is a clear indication that the distribution parameters are acceptable. Acceptable parameters help compute extreme values for different return periods for periods exceeding the observation period, i.e., beyond the year 2017 and still give a satisfactory result useful in engineering structure designs.

5.1.3 The Chi-Square and Kolmogorov-Smirnov Goodness-of-Fit Test

The hypothesis that the observations come from a Gumbel Distribution is accepted using a 5% significance level if; the computed chi-square value is less than or equal to the theoretical chi-square value. The tables (7 & 8) gives the chi-square tests for the five minutes duration for the two stations. The test is performed to determine if the data fit well to the selected distribution. Both stations have a sample size of 28 values.

Table 7: The Chi-Square Test for the 0.08 hrs Analysis NY-IRI Station

Class	Observed (O_f)	Expected (E_f)	$(O_f - E_f)$	$(O_f - E_f)^2$	$(O_f - E_f)^2/E_f$
< 10.0	10	13	-3	9	0.69230769
10.0-12.0	13	7	6	36	5.14285714
12.0-14.0	2	4	-2	4	1
14.0-16.0	1	2	-1	1	0.5
> 16.0	2	2	0	0	0
	Sum= 28	**Sum= 28**		**Sum=**	**7.33516484**

Table 8: The Chi-Square Test for the 0.08 hrs Analysis NY-Orstom Station

Class	Observed (O_f)	Expected (E_f)	$(O_f - E_f)$	$(O_f - E_f)^2$	$(O_f - E_f)^2/E_f$
< 9.0	8	13	-5	25	1.92307692
9.0-11.0	11	7	4	16	2.28571429
11.0-13.0	5	4	1	1	0.25
13.0-15.0	2	2	0	0	0
> 15.0	2	2	0	0	0
	Sum= 28	**Sum= 28**		**Sum=**	**4.45879121**

Chi-square test has critical theoretical values X^2 predetermined. For the data to obey the selected distribution, the computed X^2 has to be less than or equal to the theoretical X^2 value. For our case, the X^2 values for both stations are; - 7.34 and 4.46. For a sample size of 28 values and a significance level of 0.05%, the chi-square critical value is 41.34 (see table 23 appendix A). If the computed value is less than the critical theoretical values, the data obeys the Gumbel distribution.

$$0 \leq 7.33 \leq {X^2}_{0.05\ Iri\ Station}$$

$$0 \leq 4.4588 \leq {X^2}_{0.05\ Orstom\ Station}$$

Therefore, we accept the hypothesis that the observations data come from a Gumbel distribution at a significance level of 5%.

The results of the Kolmogorov-Smirnov test of goodness of fit showed that in 78% of the cases evaluated, had an excellent fitting. The only instances with bad fitting were the 0.25 and 0.5 hrs durations. The Kolmogorov-Smirnov test for the five minutes duration for the two rainfall stations NY-Orstom and NY-Iri results are in tables (9 & 10). Using the Kolmogorov-Smirnov test, the maximum deviation *Dn* determines if the data obeys the selected distribution or not. For the two stations NY-Iri and NY-Orstom, the computed Maximum deviation *Dn* were 0.097153 and 0.014074, respectively.

Table 9: The Kolmogorov-Smirnov Test for the 0.08 hrs analysis NY-IRI station

1	2	3	4	5	6	7	8
Interval	$\mathbf{X_0}$	$\mathbf{O_{Freq}}$	$\mathbf{Cum_{Freq}}$	$\mathbf{F_0(x)}$	**u**	$\mathbf{F_t(x)}$	$\boldsymbol{Dn = [f_t(x) - f_0(x)]}$
< 8.0	8	5	5	0.178571	-0.63405	0.151793	-0.02678
8.0-10.0	10	5	10	0.357143	0.236979	0.454295	**0.097153**
10.0-12.0	12	13	23	0.821429	1.108011	0.718769	-0.10266
12.0-14.0	14	2	25	0.892857	1.979043	0.870923	-0.02193
14.0-16.0	16	1	26	0.928571	2.850075	0.943801	0.01523

Table 10: The Kolmogorov-Smirnov Test for the 0.08 hrs analysis NY-Orstom_Stat

1	2	3	4	5	6	7	8
Interval	X_0	O_{Freq}	Cum_{Freq}	$F_0(x)$	u	$F_t(x)$	$Dn = [f_t(x) - f_0(x)]$
< 9	9	8	8	0.285714	-0.18621	0.299788	**0.014074**
9 – 11	11	11	19	0.678571	0.684818	0.604	-0.07457
11 – 13	13	5	24	0.857143	1.55585	0.809766	-0.04738
13 – 15	15	2	26	0.928571	2.426882	0.915475	-0.0131
15 - 17	17	2	28	1	3.297914	0.963715	-0.03629

The critical the value for the Kolmogorov-Smirnov test for five intervals and at a significance level of 5% is 0.563**.** The hypothesis that the data obeys Gumbel distribution is accepted at a significance level of 5 % if the computed Kolmogorov Smirnov critical values are less than the critical theoretical value (Chow et al., 1988).

Therefore, since, 0.097153 and 0.014074 are less than 0.563, the null hypothesis that our observation data comes from a Gumbel distribution is correct, at a significance level of 5%.

Both tests (Chi-Square and the Kolmogorov Smirnov) indicate that the 28 sample observations from both stations obey the Gumbel distribution.

5.1.4 Determination of flood magnitude

After the selection of the best fitting distribution, and its parameters determined, the information can further apply in estimating event magnitudes for different return periods (X_T). The distribution parameters (table 5) together with the frequency factor (see table 12) were applied to develop table (11), which presents estimated events for different return periods.

Table 11: The 0.08 hrs analysis for both stations

	NY-IRI Station			NY-Orstom Station		
T-Years	**K_T**	**$X_{(T)}$ Mm**	**I (mm/hrs)**	**K_T**	**$X_{(T)}$ Mm**	**I (mm/hrs)**
1	-0.970	8.00	100.02	-0.970	8.22	102.72
2	-0.164	10.28	128.51	-0.164	10.11	126.42
5	0.719	12.78	159.78	0.719	12.19	152.42
10	1.305	14.44	180.47	1.305	13.57	169.63
15	1.635	15.37	192.15	1.635	14.35	179.34
20	1.866	16.03	200.33	1.866	14.89	186.14
30	2.189	16.94	211.75	2.189	15.65	195.64
40	2.416	17.58	219.80	2.416	16.19	202.34
50	2.592	18.08	226.03	2.592	16.60	207.52
28	**2.134**	**16.79**	**209.81**	**2.134**	**15.52**	**194.03**
35	**2.311**	**17.29**	**216.07**	**2.311**	**15.94**	**199.23**

From table (11), a return period of *T = 1 gives a frequency factor (*K_T) value of *-0.970* and the rainfall depth for the same X_T *= 8.00 and 8.22mm* for both stations.

Table 12: Estimated frequency factor (K_T) values for different Return Periods

	Frequency Factors							
T	**1**	**2**	**5**	**10**	**20**	**30**	**40**	**50**
K_T	**-0.970**	**-0.1642**	**0.7194**	**1.3045**	**1.8658**	**2.1886**	**2.4163**	**2.5922**

From table (13), it is clear that the estimated event magnitudes seem to increase with the increasing recurrence interval. The result herein is useful for engineering structure designs since it can advise on the capacity of new structures to withstand future extreme events. Most importantly, the developed parameters can be useful in estimating future events of different return periods.

Data from both stations were analyzed using the Gumbel distribution principles to generate sub-hourly rainfall intensities for both stations tables (13 & 14). The generated results show a decreasing rainfall intensity with increase in time. Also, there is an increase in rainfall intensities with increasing return periods.

Table 13: sub-hourly intensities (mm/hr) estimates for NY–IRI station

	Return Period T							
Duration	**1**	**2**	**5**	**10**	**20**	**30**	**40**	**50**
0.08	100.02	128.52	159.79	180.49	200.34	211.77	219.82	226.05
0.17	85.61	107.15	130.79	146.43	161.44	170.08	176.16	180.87
0.25	77.41	98.63	121.92	137.34	152.13	160.64	166.64	171.27
0.5	55.47	73.16	92.57	105.41	117.74	124.83	129.83	133.69
1	31.47	44.74	59.30	68.94	78.19	83.51	87.26	90.16

Table 14: sub-hourly intensities (mm/hr) estimates for NY–Orstom station

	Return Period T							
Duration	**1**	**2**	**5**	**10**	**20**	**30**	**40**	**50**
0.08	102.73	126.43	152.43	169.64	186.15	195.65	202.35	207.52
0.17	87.19	107.93	130.68	145.74	160.19	168.50	174.36	178.89
0.25	77.98	97.15	118.18	132.11	145.46	153.15	158.57	162.75
0.5	55.79	70.01	85.60	95.93	105.83	111.53	115.55	118.65
1	32.20	43.04	54.93	62.80	70.36	74.70	77.77	80.13

The results obtained indicate that high intensities of short rainfall duration will be more severe in the future. For design purposes, this information can be very useful in determining the capacity of the structure in question. Although the results might not be an exact representation of the basin, they provide a baseline that can serve as a basis for the development of flood management strategies.

The results were plotted in a scatter diagram with duration in minutes (mins) on the x-axis and rainfall intensities (mm/hr) on the y-axis. A trend-line is then used to join points of the same return period, and the generated curves represent the sub-hourly IDF curves figures (6 & 7) for the Gountiyena basin using the observations data from both stations.

The same procedure is also applied in plotting IDF Curves (figure 8 & 9) for the given durations in tables (15 & 16)

From both tables (15 & 16), rainfall intensity magnitude is increasing with increasing return periods. Short duration events record the highest magnitudes.

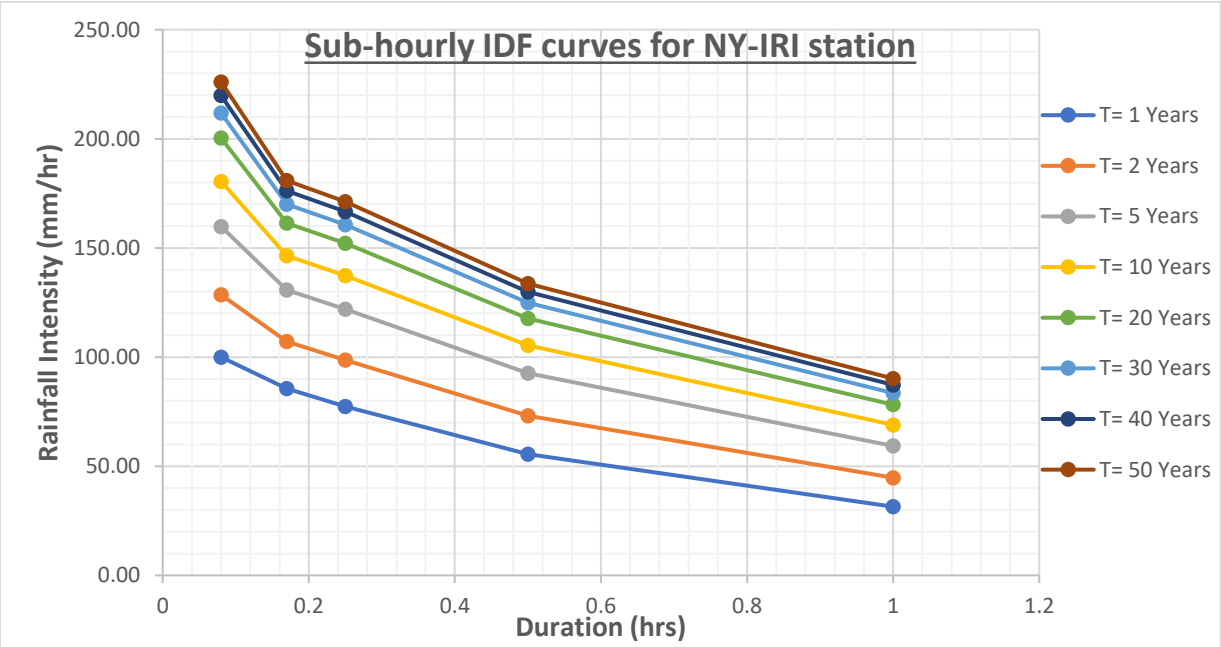

Figure 9: sub-hourly IDF estimates for the NY-IRI station

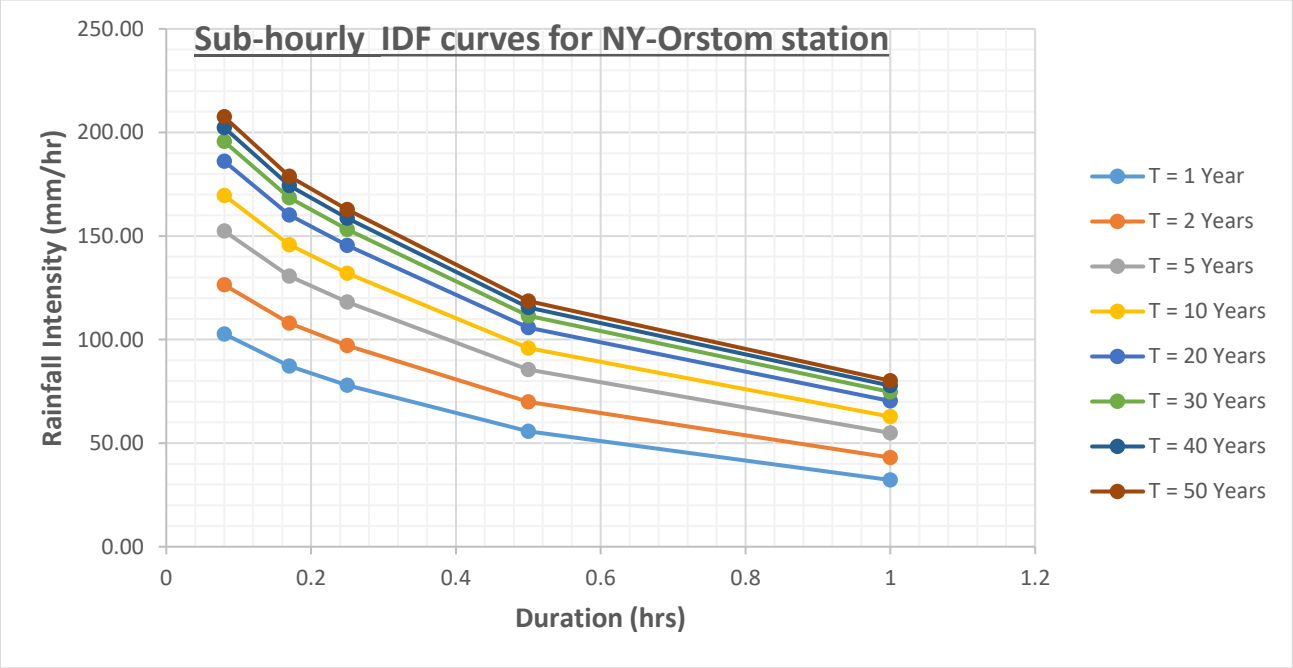

Figure 10: sub-hourly IDF estimates for the NY-Orstom station

Figure (6 & 7) present the hourly intensity duration frequency curves for the two stations. The two figures give almost similar trends with both depicting increasing intensities with increasing return

periods for short durations. Short rainfall intensities frequencies and magnitudes are projected to increase based on the results indicating an increasing flood risk.

Also, there is a decreasing trend of the rainfall intensity with increasing duration. Short durations tend to produce the highest rainfall intensities, and long duration events give the least intensities.

The following tables (15 & 16) and figures (8 & 9) represent complete IDF estimates for the study area. For readability, the plotting was done for durations up to six hours and return periods of 1, 2, 5, 10, 30, and 50. The developed curves have a wide range of applications (see section 5.1.5). Most importantly, for flood management, these curves are fundamental for any engineering structure designs. Even without discharge data, the curves can be applied to give different intensities for different return periods, which can be translated into discharge data using empirical methods such as the rational method. Most importantly, it is possible to develop future scenarios using climate change models and then apply the results to generate intensity duration frequency curves. The results will represent in-depth information regarding the behavior of short duration and long durations rainfall events.

The generated IDF estimates in this work are all in agreement with the general IDF curves properties presented in the literature review. The properties suggest that; for a given return period, high rainfall intensities allied to short durations and vice versa is also correct. Also, the generated IDF Curves, as shown in figures (9 and 10), are parallel and do not cross each other. According to the generated IDF curves, the rainfall estimates seem to increase with an increase in return period while the rainfall intensities decrease with an increase in rainfall duration on all the return periods.

Table 15: Intensity duration frequency analysis for NY-IRI station

	Return Period (T)							
Duration	**1**	**2**	**5**	**10**	**20**	**30**	**40**	**50**
0.08	100.02	128.52	159.79	180.49	200.34	211.77	219.82	226.05
0.17	85.61	107.15	130.79	146.43	161.44	170.08	176.16	180.87
0.25	77.41	98.63	121.92	137.34	152.13	160.64	166.64	171.27
0.5	55.47	73.16	92.57	105.41	117.74	124.83	129.83	133.69
1	31.47	44.74	59.30	68.94	78.19	83.51	87.26	90.16
2	16.29	24.98	34.51	40.82	46.87	50.36	52.81	54.71
6	6.09	9.34	12.91	15.28	17.55	18.85	19.77	20.48
12	3.07	4.83	6.76	8.03	9.26	9.96	10.46	10.84
24	1.60	2.52	3.53	4.20	4.84	5.21	5.46	5.67

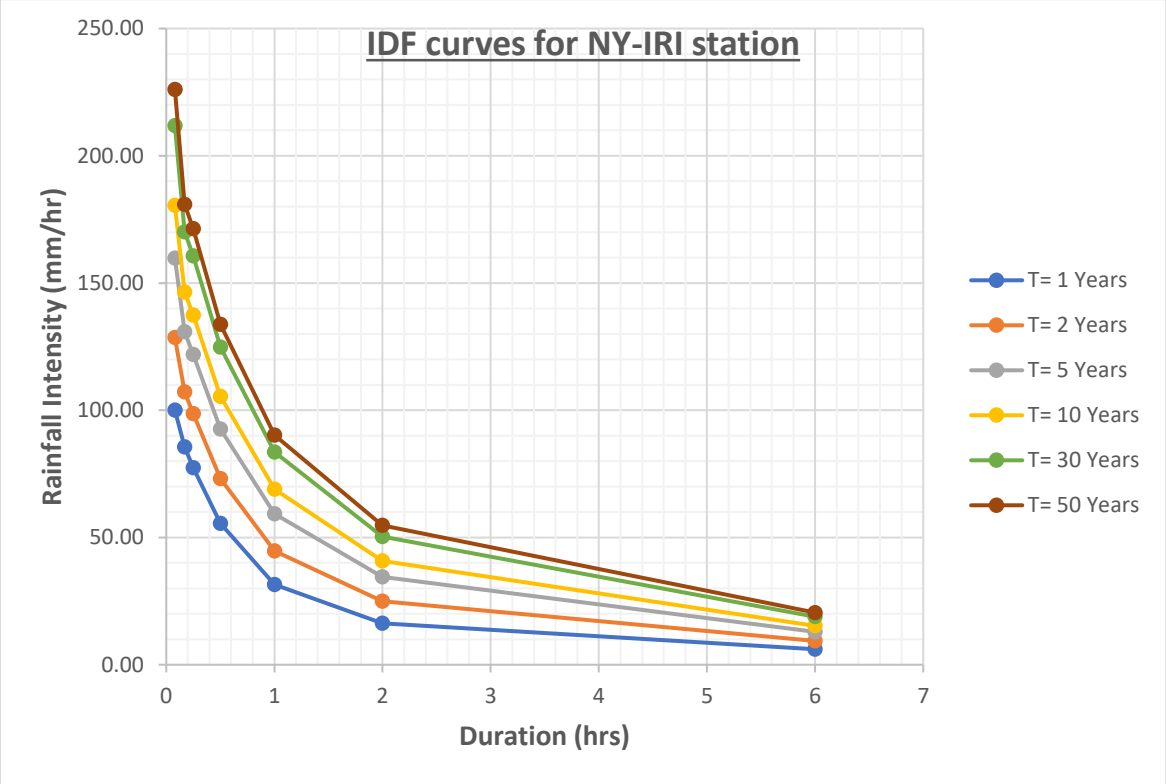

Figure 11: The IDF curves estimates NY-IRI station

Table 16: Intensity duration frequency analysis for NY-Orstom station

	Return Period T							
Duration	**1**	**2**	**5**	**10**	**20**	**30**	**40**	**50**
0.08	102.73	126.43	152.43	169.64	186.15	195.65	202.35	207.52
0.17	87.19	107.93	130.68	145.74	160.19	168.50	174.36	178.89
0.25	77.98	97.15	118.18	132.11	145.46	153.15	158.57	162.75
0.5	55.79	70.01	85.60	95.93	105.83	111.53	115.55	118.65
1	32.20	43.04	54.93	62.80	70.36	74.70	77.77	80.13
2	15.17	23.93	33.53	39.89	45.99	49.50	51.98	53.89
6	5.67	9.06	12.78	15.24	17.60	18.95	19.91	20.65
12	2.93	4.67	6.57	7.83	9.04	9.74	10.23	10.61
24	1.48	2.37	3.35	4.00	4.63	4.99	5.24	5.43

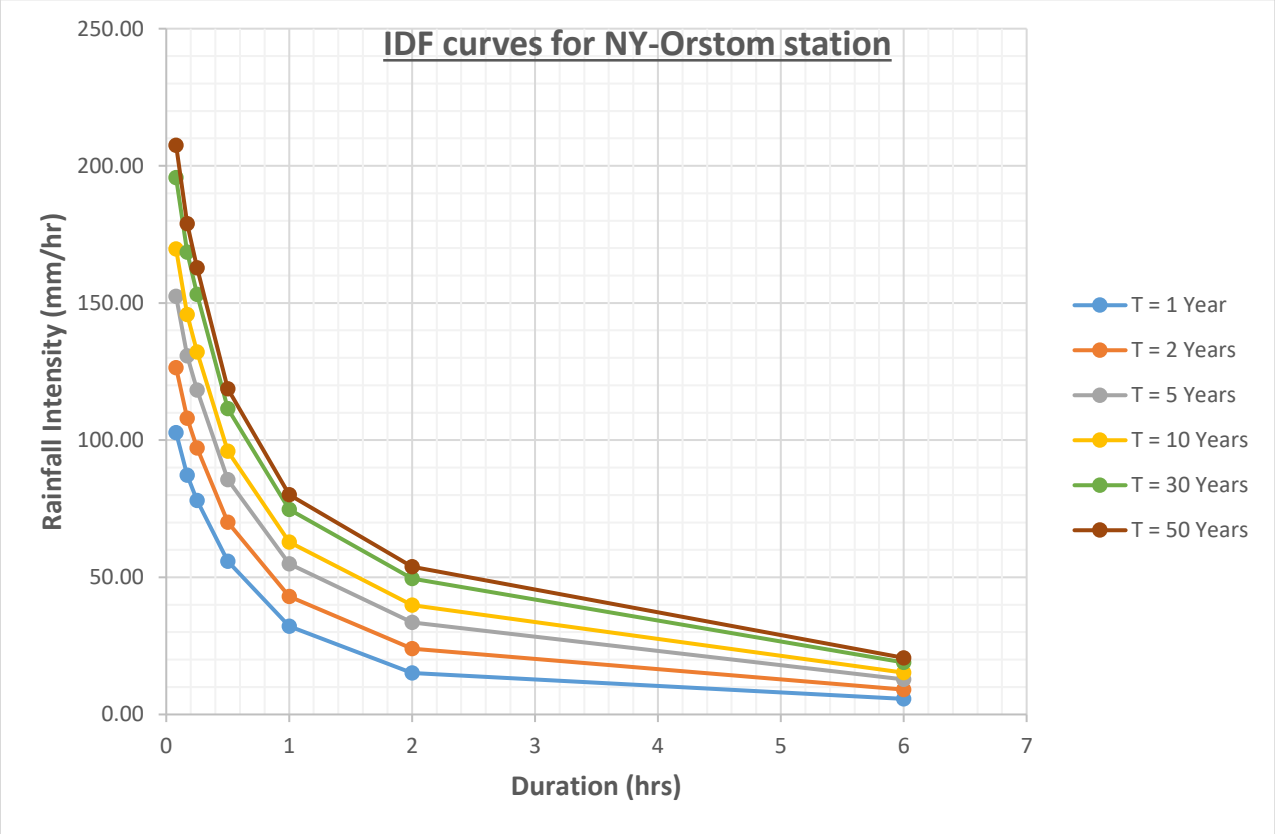

Figure 12: The IDF Curves Estimates for NY-Orstom station

5.1.5 Application of the IDF Curves

The intensity duration frequency curves obtained in this study can be useful in many sectors in the study area and beyond. For instance, some applications of these IDF curves can be the management of the municipal infrastructures such as sewers, street curb, and stormwater management ponds; the water resources management, soil conservation studies and in the land use planning. It can apply for the design of secure and economic structures for storage, control, and routing of stormwater; the construction of dams and bridges risk assessments and for roof and stormwater drainage systems design. Most importantly, the IDF curve can serve as necessary information for effective flood risk management.

5.2 Peak Discharge Estimation

5.2.1 The Rational Method

The drainage area calculated using GIS tools was 5339 hectares (53.39 km^2). The development of the rational method was targeting small basins. The application of the exact area of the catchment might lead to over-estimations. Therefore, area correction was done using the previous procedure explained (in section 4.2.1), and the new area of the catchment reduces to 2879 hectares (28.79 km^2)

Table (17) gives a detailed evaluation of the computation of the weighted runoff-coefficient, developed through the application of ArcGIS tools since the basin is not homogeneous and has different landcover types and soil cover. It indicates the different hydrologic soil groups, the land use and landcover classes, and the corresponding runoff coefficient as well as the size of the sub-areas.

The first column of the table (17) represents the different SCS soil groups (see McCuen, 1998). The soils are classified according to their infiltration capacity and based on the soil description.

The second column represents the different land-use land-cover classifications. It is essential to know the different land-use land-cover for the entire basin since it directly affects runoff generation before calculating the runoff coefficient.

Table 17: The Runoff Coefficient (C)

HYSOGr	LULC class	Runoff Coefficient (C)	Area ha	(C X Area)
C	Bare soil	0.67	9.033688	0.67
C	Wood and grass	0.42	198.7411	9.24
D	Wood and grass	0.42	9.033688	0.42
B	Grassland	0.28	668.4929	20.72
C	Grassland	0.28	153.5727	4.76
B	Wood and grass	0.42	153.5727	7.14
A	Grassland	0.28	54.20213	1.68
B	Rainfed cropland	0.21	587.1897	13.65
B	Built-up	0.89	9.033688	0.89
C	Built-up	0.89	3306.33	325.74
C	Rainfed cropland	0.21	27.10106	0.63
D	Rainfed cropland	0.21	18.06738	0.42
D	Irrigated cropland	0.29	18.06738	0.58
A	Rainfed cropland	0.21	63.23582	1.47
				Weighted coefficient (C_w) = 0.66326496

The third column gives different runoff coefficients. The runoff coefficient (C) value is estimated using the range of the storm return period, average basin slope, hydrologic soil groups, and the land-use types.

The fourth column presents the area under a specific land-use and soil group. From the column, it is evident that the built-up area takes up the most substantial portion of the study area. The last column presented the computed weighted coefficient.

Figure (10) is the hydrologic soil group map of the study area. The most dominant soil from the basin is the soil group C. the soil classification is explained deeply in section 4.21.

Table 18: Basin parameters

Area	Longest flow path (L km)	Time of concentration (T_c mins)	Lag time (T_{lag} mins)	Duration of excess rainfall (D mins)	Peak time (T_p mins)
53.39	**27.485**	153	92	20	102

5.2.1.1 Determination of peak discharge for different return periods

The duration 1.7 hours was rounded off to the nearest hour for ease in computing the rainfall intensity since we have the scale and position parameters that will assist in computing rainfall intensity for different return periods. Table (19) below gives the average discharge calculated for the period 1990 to 2017.

Table 19: Average peak discharge for the period 1990 to 2017

Average Rainfall (mm)		Intensity (mm/hr)		Q (m3/s)		Average Q
NY-Orstom	NY-IRI	NY-Orstom	NY-IRI	NY-Orstom	NY-IRI	(m3/s)
51.43	53.5	25.71	26.75	138	143	140

The results of the calculated discharges for different return periods are in the table (20) below, together with an average from both stations. The table (20) gives an estimation of probable peak discharge for return periods of 1, 2, 5, 10, 15, 20, 30, 40, and 50. These rainfall intensities were calculated using the distribution parameters for the peak time obtained for the basin.

Table 20: Peak discharge estimations for different return periods (Rational Method)

Rational Method			
	NY_Orstom	**NY_IRI**	**Average**
T-Years	**Q (m^3/s)**		**Q (m^3/s)**
1	81.13	87.09	84.11
2	127.94	133.55	130.74
5	179.30	184.51	181.90
10	213.30	218.25	215.78
15	232.49	237.29	234.89
20	245.92	250.62	248.27
30	264.68	269.24	266.96
40	277.91	282.36	280.14
50	288.14	292.51	290.33

From the results, an increase in return period results to an increase in the peak discharge. Climate change and urbanization attribute the increasing discharge for the coming years. In the recent past, many climatic projections have predicted an increasing frequency and magnitude of rainfall events.

It is difficult to tell if the results obtained present an over-estimation or an under-estimation. The confirmation is possible after some discharge and water level measurements necessary for the rating curve development. Since the essential factors are addressed, the present results represent what is likely to happen in the basin. They can be applied together with the developed IDF curves in engineering structure designs within the basin for new developments as well as the improvement of the current flood management infrastructures. However, there is a great importance of installing discharge measurements within the basin to adequately make judgments based on runoff generation within the basin for effective planning and adequate flood risk management.

In a catchment with no discharge data like the Gountiyena basin, the generated results can serve as a basis in making decisions on flood risk management especially in both structural and non-structural flood control measures including new designs and modification of the existing infrastructures.

5.2.2 The SCS-CN method

The area of the basin is 5339 hectares. However, to avoid over-estimation, the area is corrected using a correction factor, and the new area is 2879 hectares applied to calculate the Peak discharge.

Table (21) gives the weighted CN calculated in GIS based on the hydrologic soil group, land use land cover, and antecedent soil moisture

Table 21: Computation of the Composite CN for the Gountiyena Basin

Class size	CN	Soil Group	class	Area	CN X Area
1	94	C	Water body	9.033688	94
1	91	C	Bare soil	9.033688	91
22	76	C	Wood and grass	198.7411	1672
1	82	D	Wood and grass	9.033688	82
74	69	B	Grassland	668.4929	5106
17	79	C	Grassland	153.5727	1343
17	65	B	Wood and grass	153.5727	1105
6	49	A	Grassland	54.20213	294
65	78	B	Rainfed cropland	587.1897	5070
1	74	B	Built-up	9.033688	74
366	82	C	Built-up	3306.33	30012
3	85	C	Rainfed cropland	27.10106	255
2	89	D	Rainfed cropland	18.06738	178
2	89	D	Irrigated cropland	18.06738	178
7	67	A	Rainfed cropland	63.23582	469
				Composite CN	**78.671795**

The composite CN value computed was 78.671795

The basin parameters in (table 18, section 5.2.1) calculated earlier were applied in the peak discharge estimations using the SCS-CN method in the Gountiyena basin.

5.2.2.1 Peak discharge estimation

The peak discharge for the daily annual maximum values for the period 1990 to 2017 was estimated for the two stations as presented in table (22) below. The table gives an annual average for both stations, which gives an estimation of the peak discharge likely to be experienced. If there were any existing discharge data, the obtained results would be compared to determine whether it is an over-estimation or an under-estimation

Table 22: Peak discharge estimations for the period 1990 to 2017

Peak discharge estimation (Q M^3/s) using the SCS-CN Method							
	NY_Orstom	NY_IRI	Average		NY_Orstom	NY_IRI	Average
Year	(Q m^3/s)		(Q M^3/s)	Year	(Q m^3/s)		(Q M^3/s)
1990	72.41	33.01	52.71	**2004**	365.41	318.64	342.03
1991	51.28	104.39	77.84	**2005**	75.18	205.20	140.19
1992	55.84	115.87	85.86	**2006**	48.04	60.72	54.38
1993	42.48	48.77	45.63	**2007**	48.62	53.97	51.29
1994	119.12	200.81	159.97	**2008**	46.73	177.04	111.88
1995	26.81	23.80	25.30	**2009**	42.48	103.82	73.15
1996	56.96	57.96	57.46	**2010**	136.62	29.43	83.02
1997	107.46	97.16	102.31	**2011**	28.67	33.21	30.94
1998	394.77	418.25	406.51	**2012**	101.59	98.28	99.94
1999	46.85	31.18	39.01	**2013**	49.38	60.06	54.72
2000	128.62	192.67	160.64	**2014**	99.04	117.44	108.24
2001	75.21	106.98	91.10	**2015**	58.33	26.66	42.50
2002	115.28	87.99	101.63	**2016**	55.82	72.35	64.08
2003	55.29	41.88	48.58	**2017**	279.74	208.04	243.89

Table (22) gives an estimated peak discharge for the daily annual maximum values for the period 1990 to 2017. The average peak discharge for the whole period is 105 m^3/s. Both stations data does not vary significantly as it gives almost similar results for different periods. The highest recorded peak discharge was in the year 1998 with a record high of 406 m^3/s average of the two stations.

The results of the peak discharge estimated using the two methods give an idea of the probable discharge likely to be generated from the Gountiyena basin for a given rainfall event. From both methods, the results indicate an increasing trend for discharge. That means that there is a higher chance of increased frequency of flooding events. The generated results are not far from West Africa climate projections which predict an increasing trend in the frequency of rainfall events (see Akumaga & Tarhule, 2018; New et al., 2006; SYLLA et al., 2015). The current study findings confirm our research results and although there is need to perform other discharge estimations procedures and compare with the observed discharge measurements, the results cannot be ignored and can be useful in flood management and the overall engineering structure designs for development purposes.

5.3 Flood risk management practices

The study developed intensity duration frequency curves and estimated peak discharges for the period under study as well as future peak flow estimations for different return periods. The results generated can be applied as a basis in flood risk management within the Gountiyena basin. However, the design of these structures need further research to refine and extend hydrological modelling inorder to work out hydrographs for the design situations. The results from the current study are fundamental for extending existing structures but in the design and development of new structures, volumes are fundamental. It is therefore necessary to carry out an indepth analysis to come up with more concrete terms that can be applied in the design and development of these new structures.

CHAPTER 6

6 CONCLUSIONS AND RECOMMENDATIONS

6.1 Conclusion

The current research was carried out to contribute to flood risk management in the Gountiyena urban basin through the development of intensity duration frequency curves and peak discharge estimations. Three objectives directed the current study; rainfall intensity frequency analysis, estimation of probable peak discharges and the review and suggestions of best flood management options within the urban basin of the Gountiyena. The research methodology developed around the objectives and involved distribution selection, development of IDF curves and peak discharge estimations through the application of ArcGIS tools, EasyFit and Microsoft excel applications on the climate data and remote sensing data.

A theoretical probability distribution for the 5-minutes annual maximum rainfall depths for the different durations was selected using the L-moment method. The identification of the best distribution was through the application of the chi-square and the Kolmogorov-Smirnov tests for the frequency analysis. The generated IDF parameters were applied to compute estimated rainfall depths to determine the adequacy of the calculated rainfall intensities. The estimated rainfall depths were evaluated using statistical analysis against the observed values. The results indicate that the estimated rainfall-intensity duration frequency parameters sufficiently represented the rainfall characteristics of the two stations.

Two methods applied for peak discharge estimations are the Rational and the SCS-CN methods. The computation of rainfall intensities for different return periods relied on the distribution parameters for the basin`s peak time. The rational method used the calculated intensities in estimating peak discharges for different return periods. The results indicated an increasing trend for peak discharge with increasing return periods. The SCS-CN method used the daily annual maximum series for the period 1990 to 2017 to estimate peak discharges. The method generated probable peak discharges for the whole period. The result can have many applications, including hydrological modeling of the basin to further understanding its hydrology. Most importantly, they can serve as a basis in making decisions towards flood risk management within the Gountiyena basin as well as in determining capacities for different infrastructures such as bridges and drainage channels.

IDF Curves are fundamental tools for the design of drainage structures for almost all engineering projects. The obtained IDF curves and peak discharge estimations will assist engineers and urban planners in designing safe and economical flood control measures. Also, urban planners, developers, project managers, government and local authorities, and non-governmental organizations can effectively apply the results in decision making towards creating a flood risk resilience city.

However, the limited number of stations considered in this analysis can be a limit to fully decide on flood risk reduction based on the obtained results. It must be judicious to question the representativity of the two stations for the study area. We therefore suggest the instrumentation of the study area, which can later allow in-depth analysis of the flood intensity duration frequency in the basin.

6.2 Recommendations

After a careful and critical assessment of all the issues emphasized in the current study, the following suggestions act as possible solutions based on their application and efficiency in similar basins (Andjelkovic, 2001; Gomes & de Magalhaes, 2012; Carlos Eduardo Morelli Tucci, 2007; WMO, 2008, 2017a, 2017b)

i. Flood risk management is a critical issue and needs an integrated approach for successful and effective implementation. Besides, any mitigation and control measure must factor in the whole basin; otherwise, the problem will move from one geographical location to another downstream.
ii. The current study was carried out using rainfall data from two stations. The basin lacks discharge and flood data. It is therefore essential for the relevant authorities to install some gauging stations at the outlet for discharge measurements. With some flood and discharge data for the basin as well as many rainfall stations data, a more detailed and comprehensive analysis can give a more informed understanding of the basin`s hydrological behavior.
iii. There is a need for the development of an early warning system as well as awareness creation on the role of flood plains to minimize losses due to flooding. People living in flood-prone areas need relocation and the floodplain restored to minimize losses when floods occur.

iv. A practical and sustainable flood risk management plan must factor in the principles of sustainable urban flood management. Understanding the urban environment is fundamental before proposing and implementing any management option. Some of the reasons explaining the frequency of floods despite the efforts invested in controlling them are the non-consideration of the urban catchment as a whole system. Many urban flood management strategies develop on drainage design principle and evaluation and control in sections. Until we treat the whole basin one, it will be challenging to mitigate flooding but rather migrate the problem from one location to another downstream. It is due to these reasons that the study suggests the principles developed and recommended by Tucci applicable for sustainable urban flood management.

7 REFERENCES

A. M. Wasantha Lal, A. (1998). WEIGHTED IMPLICIT FINITE-VOLUME MODEL FOR OVERLAND FLOW By A. M. Wasantha Lal, *M*(September), 941–950.

Akan, A. O. (2002). Modified rational method for sizing infiltration structures. *Canadian Journal of Civil Engineering*, *29*(4), 539–542. https://doi.org/10.1139/l02-038

Akumaga, U., & Tarhule, A. (2018). Projected Changes in Intra-Season Rainfall Characteristics in the Niger River Basin, West Africa, 1983–1985. https://doi.org/10.3390/atmos9120497

AMEC Earth and Environmenta. (2001). *Georgia Stormwater Management Manual Volume 2* (First Edit). Atlanta, USA.

Andjelkovic, I. (2001). International Hydrological Programme Guidelines Non-Structural Measures in Urban Flood Management. *Technical Documents in Hydrology No.50/UNESCO*, (50), 89.

Ashley, R., Garvin, S., Pasche, E., Vassilopoulos, A., & Zevenbergen, C. (2007). *Advances in Urban Flood Management*. *Advances in Urban Flood Management*. Taylor & Francis/Balkema. https://doi.org/10.1201/9780203945988

Borga, M., Anagnostou, E. N., Blöschl, G., & Creutin, J. D. (2010). Flash floods: Observations and analysis of hydro-meteorological controls. *Journal of Hydrology*, *394*(1–2), 1–3. https://doi.org/10.1016/j.jhydrol.2010.07.048

Burlando, P., & Rosso, R. (1996). Scaling and multiscaling models of depth-duration-frequency curves for storm precipitation. *Journal of Hydrology*, *187*, 45–64.

Butler, D., & Davies, J. W. (2004). *Urban Drainage* (2nd Editio). London: Spon Press 11 New Fetter Lane, London EC4P 4EE.

Butler, D., Digman, C., Makropoulos, C., & Davies, J. W. (2018). *Urban Drainage* (4 th Edition). Boca Raton London New York: CRC Press Taylor & Francis Group.

Candela, A., Brigandì, G., & Aronica, G. T. (2014). Estimation of synthetic flood design hydrographs using a distributed rainfall-runoff model coupled with a copula-based single storm rainfall generator. *Natural Hazards and Earth System Sciences*, *14*(7), 1819–1833. https://doi.org/10.5194/nhess-14-1819-2014

Chang, H., & Bonnette, M. R. (2014). Climate change and water- - related ecosystem services : impacts of drought in California, USA, 1–19. https://doi.org/10.1002/ehs2.1254

Chang, N. (2006). Urban Flash Flood Monitoring, Mapping and Forecasting via a Tailored Sensor Network System. *2006 IEEE International Conference on Networking, Sensing and Control*, 757–761. https://doi.org/10.1109/ICNSC.2006.1673241

Chen, N. S., Yue, Z. Q., Cui, P., & Li, Z. L. (2007). A rational method for estimating maximum discharge of a landslide-induced debris flow: A case study from southwestern China. *Geomorphology*, *84*(1–2), 44–58. https://doi.org/10.1016/j.geomorph.2006.07.007

Chow, V. Te, Maidment, D. R., & Mays, L. W. (1988). *Applied Hydrology*. (B. J. Clark & J. Morriss, Eds.). McGraw-Hill, Inc.

Clark, G. (2016). Hydrologic Modeling At Ungauged Locations in Support of the Development of a Vulnerability Ranking Protocol System for Road-Stream Crossing Infrastructure.

Dawson, R. J., Speight, L., Hall, J. W., Djordjevic, S., Savic, D., & Leandro, J. (2008). Attribution of flood risk in urban areas. *Journal of Hydroinformatics*, *10*(4), 275–288. https://doi.org/10.2166/hydro.2008.054

Dhakal, N., Fang, X., Thompson, D. B., & Cleveland, T. G. (2014). Modified rational unit hydrograph method and applications. *Proceedings of the Institution of Civil Engineers - Water Management*, *167*(7), 381–393. https://doi.org/10.1680/wama.13.00032

Dupont, B. S., & Allen, D. L. (2000). *Transportation*. *Kentucky Transportation Center College of Engineering University of Kentucky Lexington, Kentucky*.

emdat. (2018). emdat_db. Retrieved January 8, 2019, from https://www.emdat.be/emdat_db/

Federal Ministry of Works. (2013). The *Federal Republic of Nigeria*. *Photogrammetric Engineering and Remote Sensing* (Vol. 75).

Filho, A. C. de P., & Pina, A. C. de. (2010). *Methods and Techniques in Urban Engineering*. Vukovar, Croatia: In-Tech.

García-Bartual, R., & Schneider, M. (2001). Estimating maximum expected short-duration rainfall intensities from extreme convective storms. *Physics and Chemistry of the Earth,*

Part B: Hydrology, Oceans, and Atmosphere, *26*(9), 675–681. https://doi.org/10.1016/S1464-1909(01)00068-5

Gerold, L. A., & David W. Watkins. (2005). Short Duration Rainfall Frequency Analysis in Michigan Using Scale-Invariance Assumptions. *Journal of Hydrologic Engineering*, 450–457.

Giannoni, F., Smith, J. A., Zhang, Y., & Roth, G. (2003). Hydrologic modeling of extreme floods using radar rainfall estimates. *Advances in Water Resources*, *26*(2), 195–203. https://doi.org/10.1016/S0309-1708(02)00091-X

Gomes, M., & de Magalhaes, L. P. C. (2012). Urban Flood Control, Simulation, and Management - an Integrated Approach. *Methods and Techniques in Urban Engineering*. https://doi.org/10.5772/9574

Greater London Authority (GLA). (2015). London Sustainable Drainage Action Plan - Draft for public consultation, 73.

Hammond, M. J., Chen, A. S., Djordjević, S., Butler, D., & Mark, O. (2015). Urban flood impact assessment: A state-of-the-art review. *Urban Water Journal*, *12*(1), 14–29. https://doi.org/10.1080/1573062X.2013.857421

Hoblit, B., Zelinka, S., Castello, C., & Curtis, D. (n.d.). Spatial Analysis of Storms Using GIS, 1–12.

Hodges, L. H., Hershfield, D. M., Washington, D. C., & Reichelderfer, F. W. (1961). *RAINFALL FREQUENCY ATLAS OF THE UNITED STATES for Durations from 30 Minutes to 24 Hours and Return Periods from I to 100 Years WEATHER BUREAU*.

Hosking, J. R. M., & Wallis, J. R. (1997). *Regional frequency analysis*. *Cambridge University Press*. https://doi.org/10.1017/cbo9780511529443.003

Hotchkiss, R. H., & McCallum, B. E. (1995). Peak Discharge for Small Agricultural Watersheds.

Hrachowitz, M., Savenije, H. H. G., Blöschl, G., McDonnell, J. J., Sivapalan, M., Pomeroy, J. W., … Cudennec, C. (2013). A decade of Predictions in Ungauged Basins (PUB)—a review. *Hydrological Sciences Journal*, *58*(6), 1198–1255. https://doi.org/10.1080/02626667.2013.803183

Hsu, M. H., Chen, S. H., & Chang, T. J. (2000). Inundation simulation for urban drainage basin with a storm sewer system. *Journal of Hydrology*, *234*(1–2), 21–37. https://doi.org/10.1016/S0022-1694(00)00237-7

Huong, H. T. L., & Pathirana, A. (2013). Urbanization and climate change impacts on future urban flooding in Can Tho city, Vietnam. *Hydrology and Earth System Sciences*, *17*(1), 379–394. https://doi.org/10.5194/hess-17-379-2013

Khan, S. I., Hong, Y., Wang, J., Yilmaz, K. K., Gourley, J. J., Adler, R. F., … Irwin, D. (2011). Satellite remote sensing and hydrologic modeling for flood inundation mapping in lake victoria basin: Implications for hydrologic prediction in ungauged basins. *IEEE Transactions on Geoscience and Remote Sensing*, *49*(1 PART 1), 85–95. https://doi.org/10.1109/TGRS.2010.2057513

Koutsoyiannis, D. (2004). Statistics of extremes and estimation of extreme rainfall: II. An empirical investigation of long rainfall records / Statistiques de valeurs extrêmes et estimation de précipitations extrêmes: II. Recherche empirique sur de longues séries de précipitations. *Hydrological Sciences Journal*, *49*(4), 37–41. https://doi.org/10.1623/hysj.49.4.591.54424

Koutsoyiannis, D., Kozonis, D., & Manetas, A. (1998). A mathematical framework for studying rainfall intensity-duration-frequency relationships. *Journal of Hydrology*, *206*, 118–135.

Koutsoyiannis, D., & Manetas, A. (1996). Simple disaggregation by accurate adjusting procedures. *Water Resources Research*, *32*(7), 2105–2117. https://doi.org/10.1029/96WR00488

Langousis, A., & Veneziano, D. (2007). Intensity-duration-frequency curves from scaling representations of rainfall. *Water Resources Research*, *43*(2), 1–12. https://doi.org/10.1029/2006WR005245

Lasagna, M., Dino, G. A., Perotti, L., Spadafora, F., De Luca, D. A., Yadji, G., … Moussa, K. (2015). Georesources and Environmental Problems in Niamey City (Niger): A Preliminary Sketch. *Energy Procedia*, *76*, 67–76. https://doi.org/10.1016/j.egypro.2015.07.848

Machiwal, D., & Jha, M. K. (2012). *Hydrologic time series analysis: Theory and practice*.

Hydrologic Time Series Analysis: Theory and Practice. https://doi.org/10.1007/978-94-007-1861-6

Maidment, D. (1996). Handbook of Hydrology.pdf.

MathWave Technologies. (2019). EasyFit - Distribution Fitting Software - Benefits. Retrieved June 22, 2019, from http://www.mathwave.com/easyfit-distribution-fitting.html

McCuen, R. H. (1998). *Hydrologic Analysis and design*. (B. Stenquist & M. Horton, Eds.), *Pearson Education, Prentice Hall Upper Saddle River, New Jersey 07458* (Second Edi). Library of Congress. https://doi.org/10.1201/9780203737538

Miguez, M. G., Mascarenhas, F. C. B., & Magalhães, L. P. C. (2005). Multifunctional landscapes for urban flood control: the case of Rio de Janeiro. *Transactions on Ecology and the Environment*, *84*, 33–52. https://doi.org/10.2495/978-1-84564-560-1/02

Mohymont, B., Demarée, G. R., & Faka, D. N. (2004). Establishment of IDF-curves for precipitation in the tropical area of Central Africa - comparison of techniques and results. *Natural Hazards and Earth System Science*, *4*(3), 375–387. https://doi.org/10.5194/nhess-4-375-2004

NASH, J. (2007). Determining Run-Off From Rainfall. *Proceedings of the Institution of Civil Engineers*, *10*(2), 163–184. https://doi.org/10.1680/iicep.1958.2025

New, M., Hewitson, B., Stephenson, D. B., Tsiga, A., Kruger, A., Manhique, A., … Town, C. (2006). Evidence of trends in daily climate extremes over southern and west Africa, *111*, 1–11. https://doi.org/10.1029/2005JD006289

Ouma, Y. O. & Tateishi, R. (2014). Urban flood vulnerability and risk mapping using integrated multi-parametric AHP and GIS: Methodological overview and case study assessment. *Water (Switzerland)*, *6*(6), 1515–1545. https://doi.org/10.3390/w6061515

Oyebande, L. (1982). Deriving rainfall intensity-duration-frequency relationships and estimates for regions with inadequate data. *Hydrological Sciences Journal*, *27*(3), 353–367. https://doi.org/10.1080/02626668209491115

Petroselli, A., & Grimaldi, S. (2018). Design hydrograph estimation in small and fully ungauged basins: a preliminary assessment of the EBA4SUB framework. *Journal of Flood Risk*

Management, *11*, S197–S210. https://doi.org/10.1111/jfr3.12193

Sayers, P., Yuanyuan, L., Galloway, G., Penning-Rowsell, E., Fuxin, S., Kang, W., … Le Quesne, T. (2013). *Flood Risk Management A Strategic Approach*. Paris, UNESCO.

Schmitt, T. G., Thomas, M., & Ettrich, N. (2004). Analysis and modeling of flooding in urban drainage systems. *Journal of Hydrology*, *299*(3–4), 300–311. https://doi.org/10.1016/S0022-1694(04)00374-9

Schoubroeck, F. van. (2010). *The remarkable history of polder systems in The Netherlands*.

Shepherd, J. M., & Burian, S. J. (2003). Detection of Urban-Induced Rainfall Anomalies in a Major Coastal City. *Earth Interactions*, *7*(4), 1–17. https://doi.org/10.1175/1087-3562(2003)007<0001:DOUIRA>2.0.CO;2

Singh, V. P., & Zhang, L. (2007). IDF Curves Using the Frank Archimedean Copula. *Journal of Hydrologic Engineering*, *12*(6), 651–662. https://doi.org/10.1061/(ASCE)1084-0699(2007)12:6(651)

Sivakumar, M. V. K. (1992). Climate change and implications for agriculture in Niger. *Climatic Change*, *20*(4), 297–312. https://doi.org/10.1007/BF00142424

Sivapalan, M., Blöschl, G., Zhang, L., & Vertessy, R. (2003). Downward approach to hydrological prediction. *Hydrological Processes*, *17*(11), 2101–2111. https://doi.org/10.1002/hyp.1425

SYLLA, M. B., GIORGI, F., PAL, J. S., GIBBA, P., KEBE, I., NIKIEMA, M., & Competence. (2015). Projected Changes in the Annual Cycle of High-Intensity Precipitation Events over West Africa for the Late Twenty-First Century, 6475–6488. https://doi.org/10.1175/JCLI-D-14-00854.1

Tiepolo, M., & Braccio, S. (2016). Flood Risk Preliminary Mapping in Niamey, Niger, (June 2017). https://doi.org/10.1515/9783110480795-013

Tingsanchali, T. (2012). Urban flood disaster management. *Procedia Engineering*, *32*, 25–37. https://doi.org/10.1016/j.proeng.2012.01.1233

Tschantz, B. A., Gangaware, T. R., & Morton, R. G. (2003). *Guide to the Selection & Design of*

Stormwater Best Management Practices (BMPs). Knoxville, Tennessee 37996.

Tucci, Carlos E. M. (2007). *Urban flood management*. *Urban Flood Management*. https://doi.org/10.1201/9780203734582

Tucci, Carlos Eduardo Morelli. (2007). *Urban Flood Management*. *World Meteorological Organization*. https://doi.org/10.1201/9780203734582

United Nation. (2018). 2018 Revision of World Urbanization Prospects | Multimedia Library - United Nations Department of Economic and Social Affairs. Retrieved December 26, 2018, from https://www.un.org/development/desa/publications/2018-revision-of-world-urbanization-prospects.html

United Nations. (2017). Volume II: Demographic Profiles (ST/ESA/SER.A/400). *World Population Prospects - The 2017 Revision, II*. https://doi.org/10.1017/CBO9781107415324.004

United Nations, Department of Economic and Social Affairs, & Population Division. (2017). *World population prospects: Data booklet 2017 Revision*. *Population Division*. https://doi.org/10.1016/j.matchemphys.2004.09.004

Veneziano, D., Langousis, A., & Furcolo, P. (2006). Multifractality and rainfall extremes: A review. *Water Resources Research*, *42*(SUPPL.), 1–18. https://doi.org/10.1029/2005WR004716

Webber, J. L., Gibson, M. J., Chen, A. S., Savic, D., Fu, G., & Butler, D. (2018). Rapid assessment of surface-water flood-management options in urban catchments. *Urban Water Journal*, *15*(3), 210–217. https://doi.org/10.1080/1573062X.2018.1424212

WMO. (2007). *FORMULATING A BASIN FLOOD MANAGEMENT PLAN A Tool for Integrated Flood Management*.

WMO. (2008). *Urban Flood Risk Management – A Tool for Integrated Flood Management Version 1.0*.

WMO. (2015). Effectiveness of Flood Management Measures. *Integrated Flood Management Tools Series*, (21).

WMO. (2017a). Community-based Flood Management. *Integrated Flood Management Tools Series*, (4).

WMO. (2017b). *Selecting Measures and Designing Strategies for Integrated Flood Management - A guidance document*.

Xu, H., Lv, D., & Fan, Y. (2012). A Pragmatic Framework for Urban River System Plan in Plain River Network Area of China, *28*, 494–500. https://doi.org/10.1016/j.proeng.2012.01.757

Yu, P. S., Yang, T. C., & Lin, C. S. (2004). Regional rainfall intensity formulas based on scaling property of rainfall. *Journal of Hydrology*, *295*(1–4), 108–123. https://doi.org/10.1016/j.jhydrol.2004.03.003

Zhang, L. (2009). Discussion of " IDF Curves Using the Frank Archimedean Copula ." *Journal of Hydrologic Engineering*, *12*(6), 108–109.

8 APPENDICES

Appendix A

Table 23: Critical Values of the Chi-Square Source Table 2-7 (McCuen, 1998)

	α							
ν	0.995	0.990	0.975	0.95	0.050	0.025	0.010	0.005
1	0.0^4393	0.0^3157	0.0^3982	0.0^3393	3.84	5.02	6.63	7.88
2	0.0100	0.0201	0.0506	0.103	5.99	7.38	9.21	10.60
3	0.0717	0.115	0.216	0.352	7.81	9.35	11.34	12.84
4	0.207	0.297	0.484	0.711	9.49	11.14	13.28	14.86
5	0.412	0.554	0.831	1.145	11.07	12.83	15.09	16.75
6	0.676	0.872	1.237	1.635	12.59	14.45	16.81	18.55
7	0.989	1.239	1.690	2.167	14.07	16.01	18.48	20.28
8	1.344	1.646	2.180	2.733	15.51	17.53	20.09	21.96
9	1.735	2.088	2.700	3.325	16.92	19.02	21.67	23.59
10	2.156	2.558	3.247	3.940	18.31	20.48	23.21	25.19
11	2.603	3.053	3.816	4.575	19.68	21.92	24.72	26.76
12	3.074	3.571	4.404	5.226	21.03	23.34	26.22	28.30
13	3.565	4.107	5.009	5.892	22.36	24.74	27.69	29.82
14	4.075	4.660	5.629	6.571	23.68	26.12	29.14	31.32
15	4.601	5.229	6.262	7.261	25.00	27.49	30.58	32.80
16	5.142	5.812	6.908	7.962	26.30	28.85	32.00	34.27
17	5.697	6.408	7.564	8.672	27.59	30.19	33.41	35.72
18	6.265	7.015	8.231	9.390	28.87	31.53	34.81	37.16
19	6.844	7.633	8.907	10.117	30.14	32.85	36.19	38.58
20	7.434	8.260	9.591	10.851	31.41	34.17	37.57	40.00
21	8.034	8.897	10.283	11.591	32.67	35.48	38.93	41.40
22	8.643	9.542	10.982	12.338	33.92	36.78	40.29	42.80
23	9.260	10.196	11.689	13.091	35.17	38.08	41.64	44.18
24	9.886	10.856	12.401	13.848	36.42	39.36	42.98	45.56
25	10.520	11.524	13.120	14.611	37.65	40.65	44.31	46.93
26	11.160	12.198	13.844	15.379	38.89	41.92	45.64	48.29
27	11.808	12.879	14.573	16.151	40.11	43.19	46.96	49.64
28	12.461	13.565	15.308	16.928	41.34	44.46	48.28	50.99
29	13.121	14.256	16.047	17.708	42.56	45.72	49.59	52.34
30	13.787	14.953	16.791	18.493	43.77	46.98	50.89	53.67

Table 24: The Kolmogorov-Smirnov Test Critical Values

SAMPLE SIZE (N)	LEVEL OF SIGNIFICANCE FOR D = MAXIMUM [$F_0(X)$ - $S_n(X)$]				
	.20	.15	.10	.05	.01
1	.900	.925	.950	.975	.995
2	.684	.726	.776	.842	.929
3	.565	.597	.642	.708	.828
4	.494	.525	.564	.624	.733
5	.446	.474	.510	.565	.669
6	.410	.436	.470	.521	.618
7	.381	.405	.438	.486	.577
8	.358	.381	.411	.457	.543
9	.339	.360	.388	.432	.514
10	.322	.342	.368	.410	.490
11	.307	.326	.352	.391	.468
12	.295	.313	.338	.375	.450
13	.284	.302	.325	.361	.433
14	.274	.292	.314	.349	.418
15	.266	.283	.304	.338	.404
16	.258	.274	.295	.328	.392
17	.250	.266	.286	.318	.381
18	.244	.259	.278	.309	.371
19	.237	.252	.272	.301	.363
20	.231	.246	.264	.294	.356
25	.210	.220	.240	.270	.320
30	.190	.200	.220	.240	.290
35	.180	.190	.210	.230	.270
OVER 35	$\frac{1.07}{\sqrt{N}}$	$\frac{1.14}{\sqrt{N}}$	$\frac{1.22}{\sqrt{N}}$	$\frac{1.36}{\sqrt{N}}$	$\frac{1.63}{\sqrt{N}}$

Table 25: Tabulated values of the runoff coefficient source: (McCuen, 1998)

TABLE 7–9 Runoff Coefficients for the Rational Formula versus Hydrologic Soil Group (A, B, C, D) and Slope Range

	A			B			C			D		
Land Use	0–2%	2–6%	6%+	0–2%	2–6%	6%+	0–2%	2–6%	6%+	0–2%	2–6%	6%+
Cultivated land	0.08[a]	0.13	0.16	0.11	0.15	0.21	0.14	0.19	0.26	0.18	0.23	0.31
	0.14[b]	0.18	0.22	0.16	0.21	0.28	0.20	0.25	0.34	0.24	0.29	0.41
Pasture	0.12	0.20	0.30	0.18	0.28	0.37	0.24	0.34	0.44	0.30	0.40	0.50
	0.15	0.25	0.37	0.23	0.34	0.45	0.30	0.42	0.52	0.37	0.50	0.62
Meadow	0.10	0.16	0.25	0.14	0.22	0.30	0.20	0.28	0.36	0.24	0.30	0.40
	0.14	0.22	0.30	0.20	0.28	0.37	0.26	0.35	0.44	0.30	0.40	0.50
Forest	0.05	0.08	0.11	0.08	0.11	0.14	0.10	0.13	0.16	0.12	0.16	0.20
	0.08	0.11	0.14	0.10	0.14	0.18	0.12	0.16	0.20	0.15	0.20	0.25
Residential lot	0.25	0.28	0.31	0.27	0.30	0.35	0.30	0.33	0.38	0.33	0.36	0.42
size 1/8 acre	0.33	0.37	0.40	0.35	0.39	0.44	0.38	0.42	0.49	0.41	0.45	0.54
Residential lot	0.22	0.26	0.29	0.24	0.29	0.33	0.27	0.31	0.36	0.30	0.34	0.40
size 1/4 acre	0.30	0.34	0.37	0.33	0.37	0.42	0.36	0.40	0.47	0.38	0.42	0.52
Residential lot	0.19	0.23	0.26	0.22	0.26	0.30	0.25	0.29	0.34	0.28	0.32	0.39
size 1/3 acre	0.28	0.32	0.35	0.30	0.35	0.39	0.33	0.38	0.45	0.36	0.40	0.50
Residential lot	0.16	0.20	0.24	0.19	0.23	0.28	0.22	0.27	0.32	0.26	0.30	0.37
size 1/2 acre	0.25	0.29	0.32	0.28	0.32	0.36	0.31	0.35	0.42	0.34	0.38	0.48
Residential lot	0.14	0.19	0.22	0.17	0.21	0.26	0.20	0.25	0.31	0.24	0.29	0.35
size 1 acre	0.22	0.26	0.29	0.24	0.28	0.34	0.28	0.32	0.40	0.31	0.35	0.46
Industrial	0.67	0.68	0.68	0.68	0.68	0.69	0.68	0.69	0.69	0.69	0.69	0.70
	0.85	0.85	0.86	0.85	0.86	0.86	0.86	0.86	0.87	0.86	0.86	0.88
Commercial	0.71	0.71	0.72	0.71	0.72	0.72	0.72	0.72	0.72	0.72	0.72	0.72
	0.88	0.88	0.89	0.89	0.89	0.89	0.89	0.89	0.90	0.89	0.89	0.90
Streets	0.70	0.71	0.72	0.71	0.72	0.74	0.72	0.73	0.76	0.73	0.75	0.78
	0.76	0.77	0.79	0.80	0.82	0.84	0.84	0.85	0.89	0.89	0.91	0.95
Open space	0.05	0.10	0.14	0.08	0.13	0.19	0.12	0.17	0.24	0.16	0.21	0.28
	0.11	0.16	0.20	0.14	0.19	0.26	0.18	0.23	0.32	0.22	0.27	0.39
Parking	0.85	0.86	0.87	0.85	0.86	0.87	0.85	0.86	0.87	0.85	0.86	0.87
	0.95	0.96	0.97	0.95	0.96	0.97	0.95	0.96	0.97	0.95	0.96	0.97

[a] Runoff coefficients for storm recurrence intervals less than 25 years.

[b]Runoff coefficients for storm recurrence intervals of 25 years or longer.

Appendix B

Table 26: The distribution parameters for the NY-Orstom station

parameters	5 mins	10 mins	15 mins	30 mins	60 mins	120 mins	360 mins	720 mins	1440 mins
Sample Mean	10.50	19.07	25.26	36.45	45.25	51.43	58.51	60.24	61.34
Sample S. dv	2.35	4.38	5.95	8.82	13.46	21.74	25.22	25.88	26.66
Position Parameter	9.43	17.07	22.55	32.43	39.11	41.52	47.01	48.43	49.18
Scale Parameter	1.91	3.55	4.83	7.16	10.92	17.63	20.46	21.00	21.62
Gumbel Mean	10.53	19.12	25.34	36.56	45.41	51.70	58.82	60.56	61.66
Gumbel S. dv	2.45	4.55	6.19	9.18	14.00	22.62	26.24	26.93	27.73
Mean of red. var.	0.56	0.56	0.56	0.56	0.56	0.56	0.56	0.56	0.56
S.dv red. var.	1.23	1.23	1.23	1.23	1.23	1.23	1.23	1.23	1.23

Table 27: The 0.08 hrs observed and expected Annual-Maxima values NY-Orstom station

Year	Rank	5 Min	P	u	XG
1991	1	16.46	0.019915	3.906259	18.43
2010	2	16.42	0.055477	2.863394	16.03
1994	3	14.01	0.091038	2.349127	14.85
2002	4	13.38	0.1266	1.999803	14.05
2012	5	12.51	0.162162	1.731997	13.43
2006	6	11.89	0.197724	1.512753	12.93
2000	7	11.56	0.233286	1.325608	12.50
1992	8	11.4	0.268848	1.161125	12.12
1998	9	11.13	0.30441	1.013368	11.78
1999	10	10.77	0.339972	0.878339	11.47
2017	11	10.76	0.375533	0.7532	11.19
2005	12	10.73	0.411095	0.635839	10.92
2016	13	10.48	0.446657	0.524624	10.66
2004	14	10.15	0.482219	0.418242	10.42
2014	15	9.84	0.517781	0.315592	10.18

1995	16	9.52	0.553343	0.215716	9.95
2001	17	9.51	0.588905	0.117737	9.73
1993	18	9.36	0.624467	0.020807	9.50
1990	19	9.04	0.660028	-0.07594	9.28
1997	20	9.01	0.69559	-0.17343	9.06
1996	21	8.82	0.731152	-0.27278	8.83
2003	22	8.61	0.766714	-0.37534	8.59
2007	23	8.6	0.802276	-0.48297	8.35
2008	24	8.5	0.837838	-0.59837	8.08
2009	25	8.23	0.8734	-0.72596	7.79
2011	26	8.06	0.908962	-0.874	7.45
2015	27	7.96	0.944523	-1.06188	7.02
2013	28	7.31	0.980085	-1.36515	6.32

Table 28: The peak discharge estimations (rational method)

NY_IRI Station					**NY_Orstom Station**				
T-Years	**Frequency factor (KT)**	**Rainfall (X mm)**	**Intensity (I mm/hr)**	**Q (m^3/s)**	**T-Years**	**Frequency factor (KT)**	**Rainfall (X mm)**	**Intensity (I mm/hr)**	**Q (m^3/s)**
1	-0.96984146	32.58	16.29	87.09	**1**	-0.969841	30.35	15.17	81.13
2	-0.16427204	49.95	24.98	133.55	**2**	-0.164272	47.86	23.93	127.94
5	0.719457416	69.02	34.51	184.51	**5**	0.7194574	67.07	33.53	179.30
10	1.304563213	81.64	40.82	218.25	**10**	1.3045632	79.79	39.89	213.30
15	1.634674959	88.76	44.38	237.29	**15**	1.634675	86.97	43.48	232.49
20	1.865810741	93.75	46.87	250.62	**20**	1.8658107	91.99	45.99	245.92
30	2.188682597	100.71	50.36	269.24	**30**	2.1886826	99.01	49.50	264.68
40	2.416317234	105.62	52.81	282.36	**40**	2.4163172	103.96	51.98	277.91
50	2.592288097	109.42	54.71	292.51	**50**	2.5922881	107.78	53.89	288.14
Average				**217.27**	**Average**				**212.31**

Table 29: The SCS-CN peak discharge estimations for the NY-Orstom station

NY_Orstom Station						
Year	**P mm**	**P - Ia**	**$(P - Ia)^2$**	**(P - Ia) + S**	**Q (mm)**	**Q (m^3/s)**
1990	54.72	40.94793	1676.733	109.80826	15.27	72.41
1991	47	33.22793	1104.095	102.08826	10.82	51.28
1992	48.74	34.96793	1222.756	103.82826	11.78	55.84
1993	43.49	29.71793	883.1554	98.57826	8.96	42.48
1994	69.78	56.00793	3136.888	124.86826	25.12	119.12
1995	36.53	22.75793	517.9234	91.61826	5.65	26.81
1996	49.16	35.38793	1252.306	104.24826	12.01	56.96
1997	66.2	52.42793	2748.688	121.28826	22.66	107.46
1998	141.8	128.0279	16391.15	196.88826	83.25	394.77
1999	45.26	31.48793	991.4897	100.34826	9.88	46.85
2000	72.63	58.85793	3464.256	127.71826	27.12	128.62
2001	55.69	41.91793	1757.113	110.77826	15.86	75.21
2002	68.61	54.83793	3007.199	123.69826	24.31	115.28
2003	48.53	34.75793	1208.114	103.61826	11.66	55.29
2004	134.71	120.9379	14625.98	189.79826	77.06	365.41
2005	55.68	41.90793	1756.275	110.76826	15.86	75.18
2006	45.73	31.95793	1021.309	100.81826	10.13	48.04
2007	45.96	32.18793	1036.063	101.04826	10.25	48.62
2008	45.21	31.43793	988.3434	100.29826	9.85	46.73
2009	43.49	29.71793	883.1554	98.57826	8.96	42.48
2010	74.99	61.21793	3747.635	130.07826	28.81	136.62
2011	37.42	23.64793	559.2246	92.50826	6.05	28.67
2012	64.36	50.58793	2559.139	119.44826	21.42	101.59
2013	46.26	32.48793	1055.466	101.34826	10.41	49.38
2014	63.55	49.77793	2477.842	118.63826	20.89	99.04
2015	49.67	35.89793	1288.661	104.75826	12.30	58.33
2016	48.73	34.95793	1222.057	103.81826	11.77	55.82
2017	113.5	99.72793	9945.66	168.58826	58.99	279.74
			Average			**99.43**

Table 30: The SCS-CN peak discharge estimations for the NY-IRI station

NY_IRI Station						
Year	**P mm**	**P - Ia**	**$(P - Ia)^2$**	**(P - Ia) + S**	**Q (mm)**	**Q (m^3/s)**
1990	39.42	25.64793	657.8163	94.50826	6.96	33.01
1991	65.24	51.46793	2648.948	120.3283	22.01	104.39
1992	68.79	55.01793	3026.973	123.8783	24.44	115.87
1993	46.02	32.24793	1039.929	101.1083	10.29	48.77
1994	92.95	79.17793	6269.145	148.0383	42.35	200.81
1995	35.04	21.26793	452.3248	90.12826	5.02	23.80
1996	49.53	35.75793	1278.63	104.6183	12.22	57.95
1997	62.95	49.17793	2418.469	118.0383	20.49	97.16
1998	147.42	133.6479	17861.77	202.5083	88.20	418.25
1999	38.59	24.81793	615.9296	93.67826	6.57	31.18
2000	90.75	76.97793	5925.602	145.8383	40.63	192.67
2001	66.05	52.27793	2732.982	121.1383	22.56	106.98
2002	59.98	46.20793	2135.173	115.0683	18.56	87.99
2003	43.24	29.46793	868.3589	98.32826	8.83	41.88
2004	123.24	109.4679	11983.23	178.3283	67.20	318.64
2005	94.13	80.35793	6457.397	149.2183	43.27	205.20
2006	50.55	36.77793	1352.616	105.6383	12.80	60.72
2007	48.03	34.25793	1173.606	103.1183	11.38	53.97
2008	86.47	72.69793	5284.989	141.5583	37.33	177.04
2009	65.06	51.28793	2630.452	120.1483	21.89	103.82
2010	37.78	24.00793	576.3807	92.86826	6.21	29.43
2011	39.51	25.73793	662.441	94.59826	7.00	33.21
2012	63.31	49.53793	2454.007	118.3983	20.73	98.28
2013	50.31	36.53793	1335.02	105.3983	12.67	60.06
2014	69.27	55.49793	3080.02	124.3583	24.77	117.44
2015	36.46	22.68793	514.7422	91.54826	5.62	26.66
2016	54.7	40.92793	1675.095	109.7883	15.26	72.35
2017	94.89	81.11793	6580.119	149.9783	43.87	208.04
			Average			**111.63**

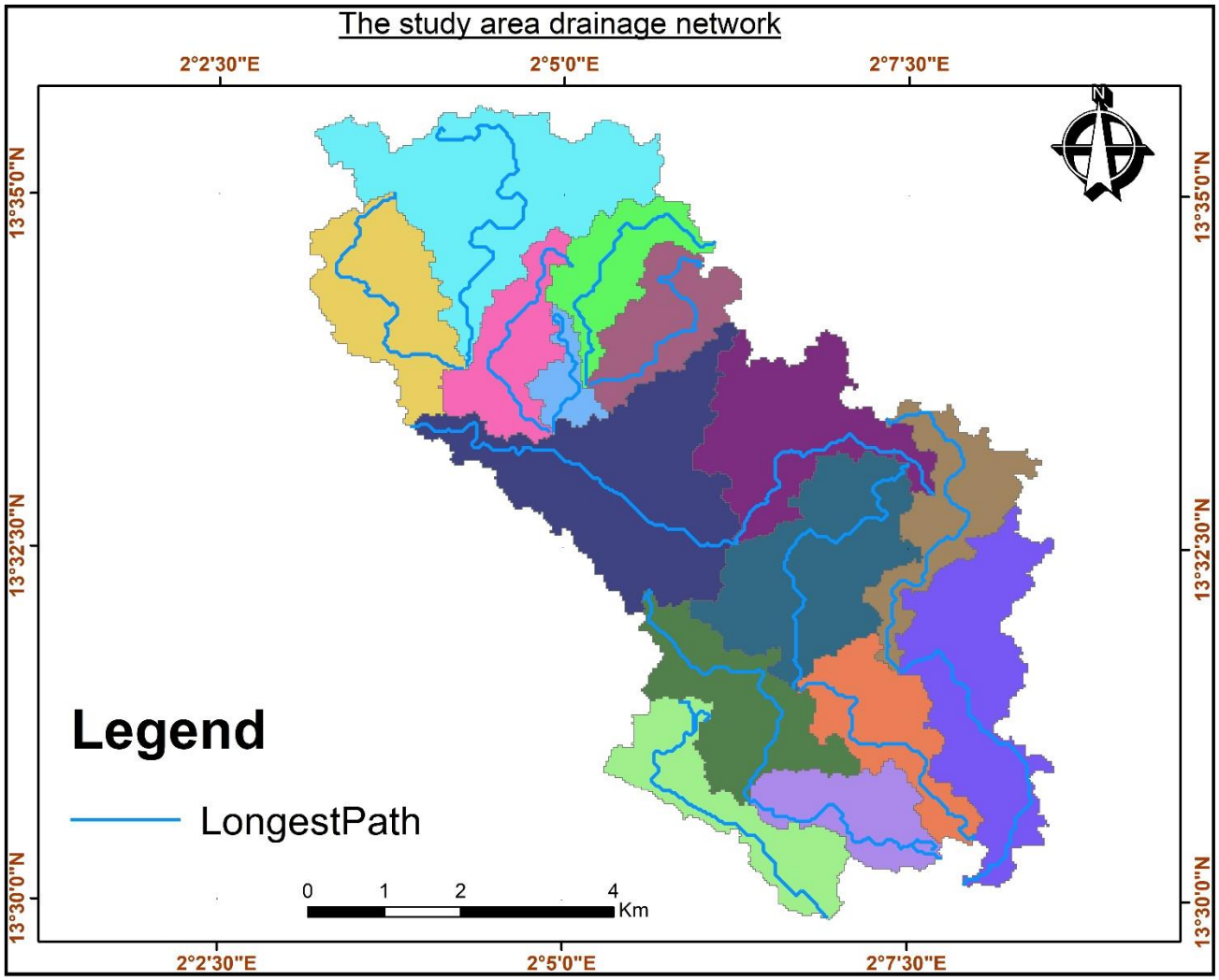

Figure 13: Longest flow path for each sub-basin

APPENDIX C

Research Grant Expenditure

Section	Section	CFA	Dzd	USD
Internet	**Internet**	**245, 000**		**440**
Insurance	**Insurance**		**8381**	**70**
Transport	**Flight change**	**48,200**		**85**
	Visa		**10,000**	**85**
			3,740	**30**
	Flight (Algiers to Niamey)			**530**
	Local Transport (Tlemcen to Algiers airport)		**3,350**	**30**
	Local Transport (Niamey airport pick up and drop)	**20,000**		**40**
	Local Transport (Algiers airport to Tlemcen)		**2,950**	**25**
Fieldwork	**Fieldwork**	**240,000**		**420**
Software	**ArcGIS Pro Software**			**110**
	X Plag checker software			**50**
Miscellaneous				**50**
Thesis Printing	**Thesis Printing**		**2750**	**25**
Total	**Total**			**1990**